Second Order Vibration of Flexible Shafts

R.E.D. Bishop and A. G. Parkinson

Email alerting service	Receive free email alerts when new articles cite this article - sign up in the box at the top right-hand corner of the article or click **here**

[1]

SECOND ORDER VIBRATION OF FLEXIBLE SHAFTS

By R. E. D. BISHOP and A. G. PARKINSON

Department of Mechanical Engineering, University College London

[Plate 1]

CONTENTS

First order (i.e. 'once per revolution') forced bending vibration of high speed flexible shafts is caused by the small defects of initial bend and lack of mass balance that are inevitably present in any rotor. It can be reduced to an acceptable level by modal balancing. Large modern alternator rotors are particularly sensitive to vibration and it has been found that, while accurate balancing is of cardinal importance, it is not sufficient to remove all vibration. There remains, in particular, second order (or 'twice per revolution') forced vibration which arises from the dual flexural rigidity that is virtually inescapable in a two-pole machine; the motion is excited by the weight of the rotor. This has now emerged as the source of considerable difficulty, largely because it can be cured only at the design stage and cannot be 'balanced'. (Certain 'trimming' modifications can be made, of course, but these present formidable problems of their own.)

A theoretical treatment of the problem is given which is much less restrictive than that previously available. An analytical basis is provided for further work of a more specific nature, should it be required. The motion is examined mode by mode and various properties of second order vibration are exposed. In particular it is shown that the polar representation that has been successfully used in the analysis of first order vibration is also of value with second order vibration. This is illustrated and confirmed with results taken from a 350 MW rotor.

INTRODUCTION

Since the Second World War, the sizes of turbo-generator rotors have increased dramatically. Figure 1 shows the relative sizes of the forgings from which these rotors are cut and it will be seen that the rotors with an output of about 750 MW that are now on the drawing board are very much longer than the 120 MW rotors that were the largest made in the 1940's. It will be seen that, as the output of these machines has been increased so the length of the rotors has increased, but not the diameters—for increases of diameter are limited by stress considerations. This increase of slenderness has meant that lower critical speeds have now to be contended with. This, in turn, has meant that sensitivity to vibration has increased.

Flexural vibration of a large alternator rotor when it is running at speed is one of the most dangerous forms of vibration met with in engineering practice. It is easy to bend a shaft when it is running at a critical speed, and a bent shaft vibrates more violently than a straight one. If a 500 MW rotor weighing more than 70 tons were to begin a violent oscillation when it was running at high speed, a colossal amount of damage could be done. The position is not improved by the very high polar moment of inertia of these rotors which ensures that rapid changes of speed cannot be made.
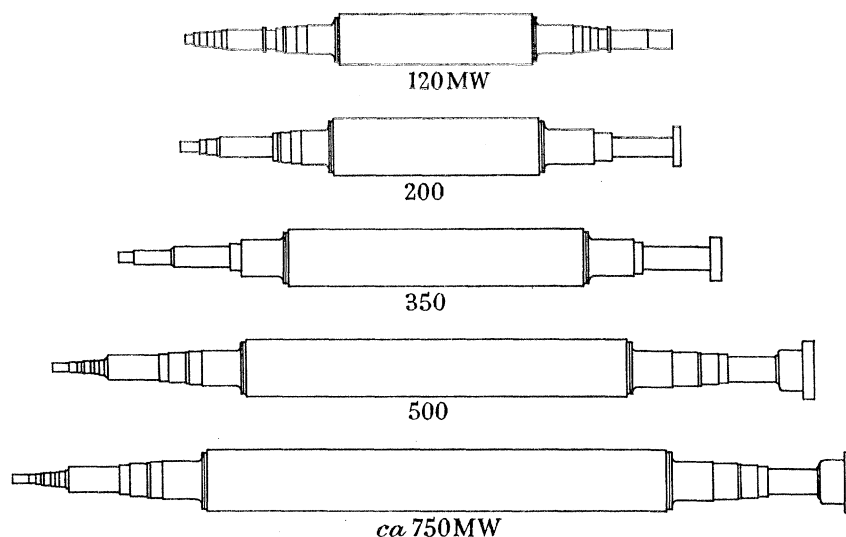

120 MW

200

350

500

ca 750MW

FIGURE 1. (By courtesy of General Electric Company, Witton.)

When supported in its two bearings, a 500 MW rotor has a sag of about 0·090 in. This sag becomes modified when the shaft rotates, though direct measurement of this modification would be extremely difficult.

Superimposed on this sag there are vibrations of the rotor. Those of most importance here are forced vibrations and they have frequencies that are related to the speed of rotation. They fall into two distinct categories:

(a) First order vibration

A first order vibration is one in which the shaft vibrates relative to non-rotating axes with a frequency in c/s numerically equal to the angular velocity of the shaft in rev/s. It is due to the small (and inescapable) defects that are left in the shaft by the processes of manufacture—defects of lack of balance and of initial lack of straightness. The rational study of first order vibration, that is forced vibration due to unbalance, may be said to have begun with the work of Jeffcott (1919). Both the motion itself and techniques of suppressing it by the process of 'balancing' have been studied intensively during the last few years, largely as a result of difficulties raised by modern alternator rotors (Lindley & Bishop 1963). The predictions of theory have been found valid in experiments on laboratory models and have also been adapted for use with alternator rotors (see Moore & Dodd 1964; Parkinson & Bishop 1965). The result is that the position is now far better than it was. By dealing with first order vibration on the basis of modal balancing theory, the position has now been reached when first order vibration is no longer a serious problem.
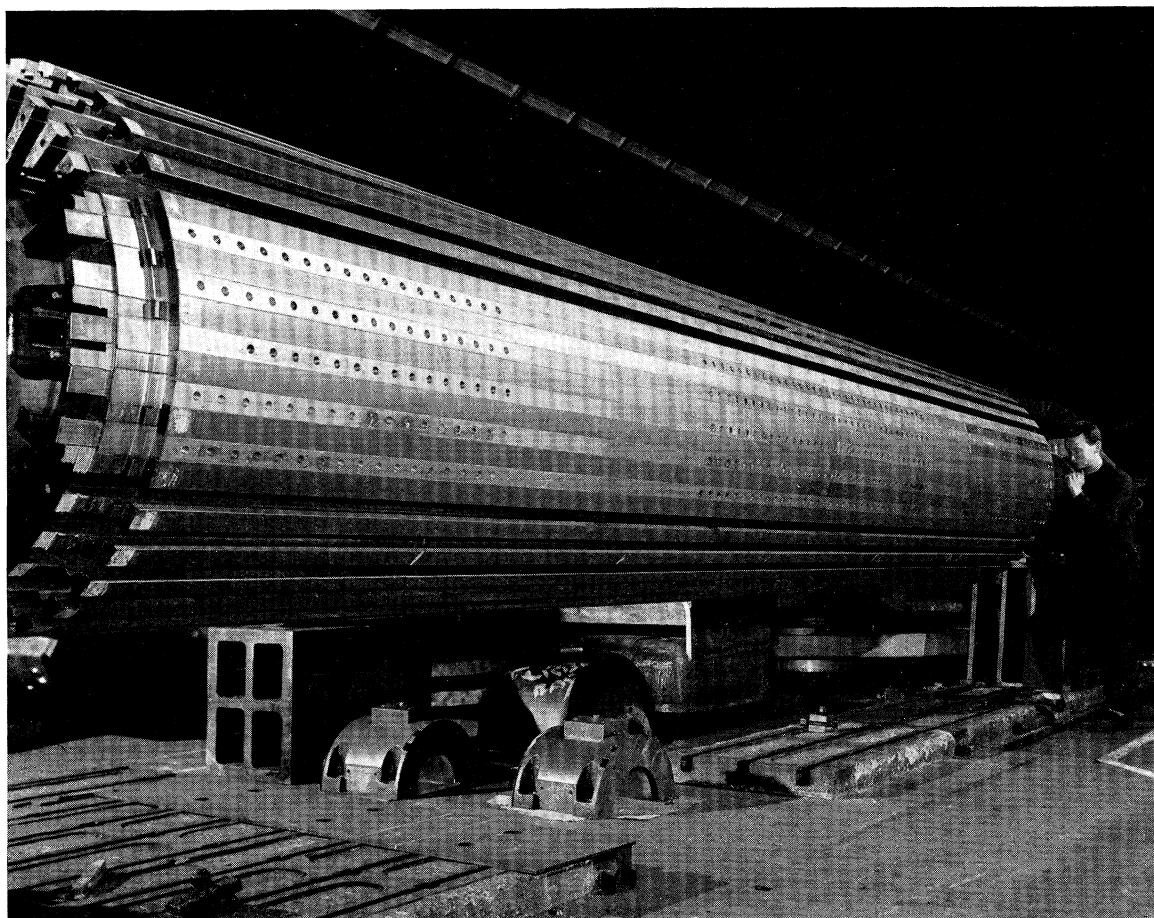
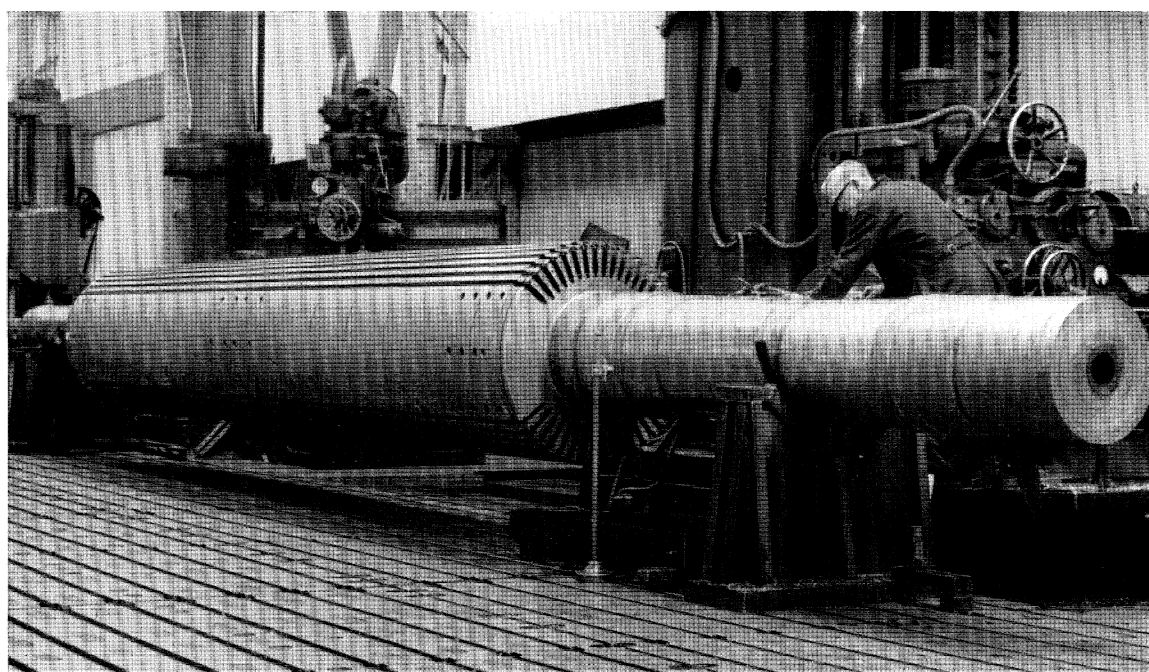FIGURE 3(*a*). (By courtesy of General Electric Company, Witton.)

FIGURE 3(*b*). (By courtesy of English Electric Company, Stafford.)

(b) Second order vibration

This motion is such that the shaft vibrates relative to stationary axes with a frequency in c/s numerically equal to twice the angular velocity of the shaft in rev/s. Now that first order vibration is relatively domesticated, second order vibration is emerging as a prime source of difficulty with some large alternators. In a very real sense, it is a more difficult one to counter than the forced vibration of 'unbalance'.

Practical balancing techniques are invariably based upon the assumption that the system being balanced possesses axial symmetry. Now second order vibration cannot be accounted for in general under this assumption of axial symmetry, although, for example, Soderberg (1932) and Biezeno & Grammel (1954) explain a form of second order vibration which, while it depends on mass unbalance, is likely to be very small. It has been observed in practice, however, that serious second order vibration is independent of mass unbalance. This vibration is displayed by a shaft possessing a slight lack of axial symmetry, the motion being caused by the weight of the shaft.
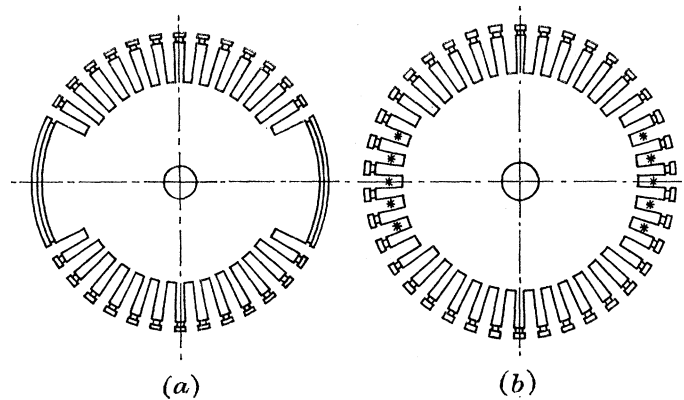

(a)   (b)

FIGURE 2. (By courtesy of General Electric Company, Witton.)

It would in fact be very difficult accurately to design an alternator rotor so as to have axial symmetry in a dynamical sense. The rotor is, in effect, a large rotating electromagnet, having a north pole and a south pole on opposite sides of the rotor and having slots cut in it in which copper conductors are embedded to provide the magnetic field. The cross-section of a 120 MW alternator rotor after slotting is shown in figure 2(a). It is clear from the figure that the flexural rigidity of the shaft is unlikely to be the same for bending about the horizontal and the vertical neutral axes, even after copper conductors and steel wedges have been placed in the slots. In attempts to equalize these rigidities, one of two schemes is usually adopted. In the first, the pole faces are slotted as shown in figure 2(b). In order to maintain the magnetic flux density, the slots in the pole faces are filled with steel bars that are wedged in. The second technique is to build a rotor in the manner of figure 2(a) and then to cut lateral slots across the poles at intervals along the length of the rotor. Figure 3(a) plate 1, shows a rotor of the first type and figure 3(b) shows one of the second.

The possibility of second order vibration has been recognized and a body of theory exists (see, for instance, Soderberg 1932; Robertson 1933; Smith 1933; Taylor 1940; Laffoon & Rose 1940; Mortensen & Ryan 1940; Dick 1948; Tondl 1958 and Hull 1961). This theory is based mainly on an adaptation of the original theory of Jeffcott. It postulates a massless

shaft having unequal flexibilities in two directions at right angles and carrying a mass at its mid-section as shown in figure 4. But while a great deal of insight has been obtained from this model, it is not really sufficient for the needs of the engineer, and a more complete picture is needed.

Fundamentally, the shortcomings of previous theory can be traced back to the violence of the idealization upon which it is based. The nature of the speed-dependent sag of a real rotor and the relative importance of the amplitude of second order vibration and of the sag are typical matters which cannot be elucidated in terms of previous theory. Again, if a shaft has unequal flexural rigidities, how must the usual process of modal balancing be modified? Questions of this sort are quite basic and answers to them are not in general available on the basis of previous theory. In fact, when he is confronted with detailed measurements obtained for the whole range of running speed, the analyst has a difficult task of interpretation to perform. Positive identification of an amplitude peak may not be easy and a decision as to what should be done about it may be difficult to reach.
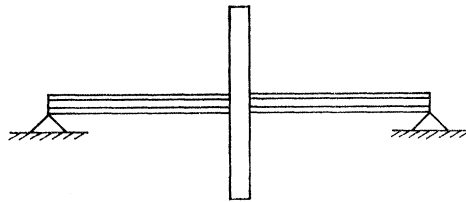

FIGURE 4.

The purpose of this paper, then, is to put the theory of second order vibration on a broader basis. It does so by relaxing the violent idealization of the model shown in figure 4. A less restrictive theory has been advanced in a few papers (see, for example, Kellenberger 1955; Tondl 1958; Dimentberg 1961), but none of these has attempted a modal analysis. They have usually presented a closed solution to the problem of a uniform, flexible shaft supported in self-alining bearings. Dimentberg, however, does discuss the effects of damping. The present paper provides answers to questions of the type referred to above and shows how other questions can be tackled if the need should arise. Finally, a technique for displaying results is suggested and illustrated. When suitably developed, this technique should provide the vibration analyst with a convenient means of interpreting observed vibrations.

Alternator rotors are supported in plain bearings and it is undoubtedly true that these bearings present unequal dynamical flexibilities in the vertical and horizontal directions. Now asymmetry of the bearings introduces further modifications to the vibration of a rotor, including the second order vibration. This form of asymmetry, however, cannot by itself *cause* second order vibration. Therefore, since bearing asymmetry seriously complicates the problem, all consideration of it is left out in the present treatment. The motion of a shaft with axial symmetry supported in asymmetric bearings has been examined and will be reported elsewhere (Parkinson 1965). A modal analysis of the combined effects of both forms of asymmetry is very complicated. An indication of this is given by the treatment of the simple rotor of figure 4, when supported in asymmetric bearings (see, for example, Foote, Poritsky & Slade 1943; Smith 1933).

Notation

The notation of other than local importance is as follows:

A_r, B_r, C_r, D_r constants partly determining amplitude of vibration due to weight of shaft (see equation (34))

$\overline{A}_r \qquad = \frac{1}{4}ig_r\left(\dfrac{\omega_r'^2 - \omega_r^2}{\omega_r'^2 + \omega_r^2}\right)$

$A\rho$ function of x representing mass per unit length of non-uniform shaft

$(A\rho)_0$ reference value of mass per unit length, equals $A\rho$ for uniform shaft

a, a' components of eccentricity of mass centre of any cross-section of shaft parallel to directions OU, OV (functions of x)

$\overline{a} \qquad = a + ia'$

a_r, a_r' components of a, a' in rth pair of principal modes of shaft

$\overline{a}_r \qquad = a_r + ia_r'$

$\overline{a}_r^* \qquad = a_r - ia_r'$

b_e, b_i coefficients of external and internal viscous damping respectively

D_1, D_2, D_3 points at ends of 'resonance diameters' in figures 14 and 15

EI flexural rigidity of shaft in OXU plane

$(EI)'$ flexural rigidity of shaft in OXV plane

E_r function of Ω introduced in equation (27)

F_r constant introduced in equation (27)

g acceleration due to gravity

g_r component of g in rth pair of modes (see equation (36))

$K \qquad = (EI)'/EI$ for non-uniform shafts, if this ratio is *constant*

l length of shaft

$OXYZ$ axes fixed in space such that OX is horizontal and parallel to undeflected axis of bearings, OY is horizontal and OZ is vertically upwards

$OXUV$ axes rotating with shaft such that OXU and OXV coincide with the principal planes of minimum and maximum flexural rigidity respectively

P_r, Q_r complex constants describing distortion of shaft due to its weight (see equations (37))

R_r see equation (71)

t time variable

u, u' displacements of shaft parallel to axes OY and OZ respectively

v, v' displacements of shaft parallel to axes OU and OV respectively

v_0, v_0' components of initial bend of shaft parallel to axes OU and OV respectively

x distance along shaft

Z normalizing factor for characteristic functions (see equation (7))

$\alpha_r, \alpha_r', \beta_r, \beta_r'$ coefficients in the expressions for the principal modes of free vibration of non-rotating shaft

6   R. E. D. BISHOP AND A. G. PARKINSON

$\bar{\epsilon}_r$ component of initial bend in rth pair of modes (see equation (63))

ζ_r $= \tan^{-1}\left(\dfrac{2\mu_r\omega_r^*\Omega}{\omega_r^{*2}-\Omega^2}\right)$

η $= v + iv'$

η^* $= v - iv'$

η_r component of η in rth pair of modes (see equation (23))

θ_r $= \tan^{-1}(a_r'/a_r)$, angular location of plane of unbalance in rth pair of modes relative to axes $OXUV$

λ degree of asymmetry of cross-section of uniform shaft (see figure 7)

λ_r see equation (75)

μ_r, ν_r rth damping factors for external and internal damping respectively

$\bar{\mu}_r$ minimum value of μ_r for which shaft is stable in rth pair of modes at speeds between ω_r and ω_r'

ξ $= u + iu'$

$\xi^{(1)}$ $= \sum\limits_{r=1}^{\infty} Q_r \phi_r(x)$

$\xi^{(2)}$ $= \sum\limits_{r=1}^{\infty} P_r \phi_r(x)\, e^{2i\Omega t}$

ξ_r component of ξ in rth pair of modes (see equation (38))

$\xi_r^{(1)}, \xi_r^{(2)}$ components of $\xi^{(1)}$ and $\xi^{(2)}$ respectively in rth pair of modes (see equations (51) and (52))

σ_r $= \tan^{-1}\left(\dfrac{\mu_r\omega_r^*\Omega}{\Omega_r^2-\Omega^2}\right)$

$\phi_r(x)$ rth characteristic function

Ω angular velocity of shaft

Ω_r $= \omega_r\omega_r'/2\omega_r^*$

ω_r rth natural frequency of non-rotating shaft in flexure in OXU plane

ω_r' rth natural frequency of non-rotating shaft in flexure in OXV plane

ω_r^* see equations (16)

EQUATIONS OF MOTION

Following the earlier analysis of systems with axial symmetry (Bishop 1959) let OX represent the undeflected axis of the bearings, assumed to be horizontal. The axes $OXYZ$ are formed by defining two mutually orthogonal fixed directions OY and OZ in a plane perpendicular to OX, such that OY is horizontal and OZ is vertically upwards. Similarly, let $OXUV$ be a set of rectangular axes such that the directions OU and OV rotate about the axis OX with the angular velocity Ω of the shaft.

At any section along the axis OX the shaft has two orthogonal principal planes of flexure, and it will be assumed that these principal planes are the same at all sections along the axis OX. The directions OU and OV will be associated with these principal planes of flexure, in fact with the planes of minimum and maximum flexural stiffness respectively (as indicated

in figure 5 which shows a cross-section of the shaft). The deflexion of the centre E of the shaft at any section x along OX may be expressed by coordinates $u(x, t)$ and $u'(x, t)$ relative to the fixed directions OY and OZ respectively. Alternatively this deflexion may be described by coordinates $v(x, t)$ and $v'(x, t)$ measured along the rotating axes OU and OV respectively (see figure 5). The two sets of coordinates are related by the following transformations:

$$\left.\begin{array}{l} u = v \cos \Omega t - v' \sin \Omega t, \\ u' = v \sin \Omega t + v' \cos \Omega t. \end{array}\right\} \tag{1}$$

In the analysis of shaft systems with axial symmetry, both sets of coordinates are used; some particular motion may be described more simply with one than with the other. For present purposes the equations of motion are most readily solved in terms of the coordinates v and v', no matter which part of the motion is being discussed. If it is required, the distortion of the shaft relative to the fixed axes $OXYZ$ can always be found through equation (1).
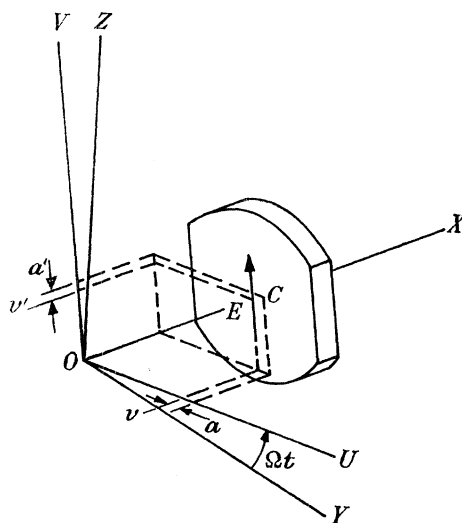

FIGURE 5

Let the flexural rigidities of the shaft at any axial section be EI and $(EI)'$, in the planes OXU and OXV respectively. In general, the cross-section of a shaft varies along its length so that these rigidities are functions of x. The displacement of the point E on the axis of the shaft is described by the equations,

$$\ddot{v} + \left[\frac{b_e + b_i}{(A\rho)_0}\right] \dot{v} - \Omega^2 v + \frac{1}{A\rho} \frac{\partial^2}{\partial x^2}\left[EI \frac{\partial^2 v}{\partial x^2}\right] - 2\Omega \dot{v}' - \frac{b_e}{(A\rho)_0} \Omega v' = a\Omega^2 + \frac{1}{A\rho} \frac{\partial^2}{\partial x^2}\left[EI \frac{\partial^2 v_0}{\partial x^2}\right] - g \sin \Omega t, \tag{2}$$

and

$$\ddot{v}' + \left[\frac{b_e + b_i}{(A\rho)_0}\right] \dot{v}' - \Omega^2 v' + \frac{1}{A\rho} \frac{\partial^2}{\partial x^2}\left[(EI)' \frac{\partial^2 v'}{\partial x^2}\right] + 2\Omega \dot{v} + \frac{b_e}{(A\rho)_0} \Omega v$$

$$= a'\Omega^2 + \frac{1}{A\rho} \frac{\partial^2}{\partial x^2}\left[(EI)' \frac{\partial^2 v_0'}{\partial x^2}\right] - g \cos \Omega t. \tag{3}$$

Apart from the allowance for unequal stiffnesses, the formulation of these equations has been described before (Gladwell & Bishop 1959). Through the coefficients b_e and b_i, allowance is made for external and internal viscous damping forces which act at the centre E of any section of the shaft. The departure of the mass centre, C, at any cross-section of the

8   R. E. D. BISHOP AND A. G. PARKINSON

shaft from the geometric centre E is represented by the components $a(x)$ and $a'(x)$, as shown in figure 5. Any initial lack of straightness in the shaft is denoted by the initial bend $v_0(x)$ and $v_0'(x)$. The remaining symbols are briefly explained in the list of notation.

If the shaft under consideration were vertical, then the undeflected bearing axis OX would also be vertical. In this event, a set of rotating axes $OXUV$ can still be defined and the equations of motion set up in terms of the coordinates v, v' as before. In fact the resulting expressions would be identical to equations (2) and (3), except that the terms $g \sin \Omega t$ and $g \cos \Omega t$ would be missing. The flexural vibration of a vertical shaft, therefore, is not affected by the weight force and the solutions of equations (2) and (3) which are arrived at later in this paper must be interpreted with g set equal to zero. We have ignored here the force which would be applied to a vertical shaft along its axis by the bearings. This force would lower the critical speeds if the weight were borne at the bottom end of the shaft, and raise them if the shaft were suspended from the top.

The solution of the equations of motion for systems with axial symmetry depended upon the existence of distinct principal modes of free vibration of the shaft in the absence of damping and rotation. The modes are determined by their natural frequences and characteristic functions—the latter defining the modal shapes. The principal modes are orthogonal in the sense that a vibration in one mode is independent of that in any other. Further, owing to axial symmetry, the principal modes and natural frequencies of any shaft are the same in all planes through the geometric axis of the shaft. On this basis the equations of motion can be solved for each principal mode in turn and the total vibration determined as the sum of the component displacements so found.

In general, if a shaft has distinct principal planes of flexure, then the principal modes of free vibration in these two planes are different. If it is allowed for, this introduces considerable complication into the analysis and (so far as the authors are aware) it has effectively prevented all progress in arriving at a really general theory. For the present, the simplifying assumption will be retained, that the principal modes of vibration in the OXU and OXV planes are of the same form so that a single set of characteristic functions serves for both. It may be noted that this simplification is justified if two restrictions are imposed on the shaft and its bearings:

(a) The analysis is confined to a shaft whose cross-section remains constant along its length; that is the flexural rigidities EI and $(EI)'$ are independent of the distance x along the axis OX. In these circumstances the mass per unit length of the shaft $A\rho = (A\rho)_0$, a constant. A slight relaxation in this restriction can be achieved by allowing the cross-section of the shaft to vary, such that $(EI)' = K(EI)$ where K is constant.

(b) The constraints of the bearings are represented by ideal end conditions, so that the shaft can be treated as having 'clamped', 'pinned', 'sliding' or 'free' ends.

As a result of these simplifications the principal modes in the principal planes of flexure still have distinct natural frequencies, but the characteristic functions in the two directions are identical. Thus free vibration in the principal modes of the non-rotating shaft in the absence of damping are described by

$$v = \phi_r(x) \left[\alpha_r \cos \omega_r t + \beta_r \sin \omega_r t\right], \\ v' = \phi_r(x) \left[\alpha_r' \cos \omega_r' t + \beta_r' \sin \omega_r' t\right], \quad (r = 1, 2, \ldots), \quad (4)$$

where α_r, α_r' ... are constants. The characteristic functions $\phi_1(x)$, $\phi_2(x)$, ... are defined by the boundary conditions at the bearings and must satisfy the following differential equations:

$$\frac{EI}{A\rho}\frac{\mathrm{d}^4\phi_r}{\mathrm{d}x^4} = \omega_r^2\,\phi_r(x),$$

$$\frac{(EI)'}{A\rho}\frac{\mathrm{d}^4\phi_r}{\mathrm{d}x^4} = \omega_r'^2\phi_r(x);$$

or

$$\frac{1}{A\rho}\frac{\mathrm{d}^2}{\mathrm{d}x^2}\left[EI\frac{\mathrm{d}^2\phi_r}{\mathrm{d}x^2}\right] = \omega_r^2\,\phi_r(x),$$

$$\frac{1}{A\rho}\frac{\mathrm{d}^2}{\mathrm{d}x^2}\left[(EI)'\frac{d^2\phi_r}{\mathrm{d}x^2}\right] = \frac{K}{A\rho}\frac{\mathrm{d}^2}{\mathrm{d}x^2}\left[EI\frac{\mathrm{d}^2\phi_r}{\mathrm{d}x^2}\right] = \omega_r'^2\phi_r(x). \tag{5}$$

The latter pair of equations refer to the simple form of non-uniformity described in restriction (a) above.

Thus the natural frequencies for the two principal planes are related by

$$\frac{\omega_r^2}{\omega_r'^2} = \frac{EI}{(EI)'} < 1. \tag{6}$$

The analysis that follows is confined to uniform shafts, so that the principal modes are orthogonal in the sense that

$$\int_0^l \phi_r(x)\,\phi_s(x)\,\mathrm{d}x = \begin{cases} 0 & (r \neq s), \\ Z, \text{ a constant} & (r = s). \end{cases} \tag{7}$$

This relation is a direct consequence of the equations (5) and the end conditions. If desired, it could very easily be rephrased for shafts of non-uniform cross-section such that

$$(EI)' = K(EI),$$

where K is constant. For the simple shafts being considered here the functions $\phi_r(x)$ have been tabulated (Bishop & Johnson 1960).

On the basis of the above simplifications it is possible to solve the equations of motion (2) and (3) in terms of orthogonal characteristic functions.

Vibration of a uniform, axially asymmetric shaft in 'ideal' bearings

Although the main subject of this paper is the second order ('twice-per-revolution') vibration of a horizontal axially asymmetric rotating shaft due to its own weight, it will be worth while briefly to examine the free vibration and the forced vibration due to unbalance. There are several distinct features of these vibrations which will help to identify the presence of axial asymmetry. Thus there will be evidence, independent of the actual twice-per-revolution vibration, to suggest asymmetry in the shaft. (A more complete discussion of these motions, and also of the balancing problem, is given elsewhere (Taylor 1940; Parkinson 1965).)

The equations of motion of a uniform shaft may be derived from equations (2) and (3) in the form

$$\ddot{v} + \left[\frac{b_e+b_i}{A\rho}\right]\dot{v} - \Omega^2 v + \frac{EI}{A\rho}\frac{\partial^4 v}{\partial x^4} - 2\Omega\dot{v}' - \frac{b_e}{A\rho}\Omega v' = a\Omega^2 - g\sin\Omega t, \tag{8}$$

$$\ddot{v}' + \left[\frac{b_e+b_i}{A\rho}\right]\dot{v}' - \Omega^2 v' + \frac{(EI)'}{A\rho}\frac{\partial^4 v'}{\partial x^4} + 2\Omega\dot{v} + \frac{b_e}{A\rho}\Omega v = a'\Omega^2 - g\cos\Omega t. \tag{9}$$

For brevity the possibility of initial lack of straightness (or 'elastic unbalance'), as represented by the terms containing v_0 and v_0' in equations (2) and (3), has been disregarded in forming equations (8) and (9). The treatment of this defect is very similar to that of mass unbalance, and in any case forced vibration due to want of balance is not the main subject of this investigation.

An alternative form of the equations of motion (8) and (9) which is often useful is obtained by introducing the complex vector notation,

$$\eta = v + iv'. \tag{10}$$

Expressions (8) and (9) can then be replaced by the single equation

$$\ddot{\eta} + \left[\frac{b_e + b_i}{A\rho}\right]\dot{\eta} - \Omega^2 \eta + \frac{1}{2}\left[\frac{EI + (EI)'}{A\rho}\right]\frac{\partial^4 \eta}{\partial x^4} + \frac{1}{2}\left[\frac{EI - (EI)'}{A\rho}\right]\frac{\partial^4 \eta^*}{\partial x^4}$$
$$+ 2i\Omega\dot{\eta} + \frac{ib_e}{A\rho}\Omega\eta = \bar{a}\Omega^2 - ig\,e^{-i\Omega t}, \tag{11}$$

where

$$\bar{a} = a + ia' \quad \text{and} \quad \eta^* = v - iv'. \tag{12}$$

As the equations of motion (8) and (9) or (11) are linear, the various forms of vibration can be investigated independently and the total vibration found as a linear combination of the separate solutions. Thus the free vibration of the system is represented by the solution of equations (8) and (9) with the right hand sides zero—that is, by the complementary functions of the differential equations of motion. Similarly, the effect of unbalance can be examined by omitting the terms due to the weight of the shaft and finding the particular integrals of the resulting differential equations.

(a) *Free vibration*

A complete solution for the free vibration of the asymmetric shaft is complicated,† but we are mainly interested in the possibility of this free vibration being unstable. If equations (8) and (9) are solved for free vibration, and the Routh stability criteria are applied to the result, it is found that the rotating shaft is stable in the rth pair of modes at all shaft speeds Ω for which all the following conditions are satisfied:

$$(\Omega^2 - \omega_r^2)(\Omega^2 - \omega_r'^2) + 4\mu_r^2 \omega_r^{*2}\Omega^2 > 0, \tag{13}$$

$$(\mu_r + \nu_r)\omega_r^{*2} + (\mu_r - \nu_r)\Omega^2 > 0, \tag{14}$$

$$[(\mu_r + \nu_r)^2 \omega_r^{*2} - \nu_r^2 \Omega^2][(\mu_r + \nu_r)^2 \omega_r^{*2} + \nu_r^2 \Omega^2] + \tfrac{1}{16}(\mu_r + \nu_r)^2(\omega_r'^2 - \omega_r^2)^2 > 0, \tag{15}$$

where

$$\left.\begin{aligned} 2\omega_r^{*2} &= \omega_r^2 + \omega_r'^2, \\ b_e/A\rho &= 2\mu_r\omega_r^*, \\ b_i/A\rho &= 2\nu_r\omega_r^*. \end{aligned}\right\} \tag{16}$$

It will be noticed that inequality (13) does not contain the internal damping factor ν_r, whereas (14) and (15) do. These conditions are thus of two sorts.

If the shaft has axial symmetry (that is $\omega_r = \omega_r^* = \omega_r'$), condition (15) reduces to the standard form

$$\Omega < \omega_r[1 + \mu_r/\nu_r] \tag{17}$$

---

† The special case of an undamped uniform pinned-pinned shaft has been solved by Johnson (1952), Tondl (1958) and Dimentberg (1961).

(see, for example, Bishop 1959). Under these circumstances condition (14)† predicts instability at a speed equal to, or higher than, that determined by inequality (17) and relation (13) is aways satisfied.

For a shaft with axial asymmetry inequalities (14) and (15) are harder to interpret, but at least they show that the shaft is stable in the rth pair of modes for all shaft speeds less than Ω'_r (except where restricted by condition (13)), where Ω'_r satisfies the inequality

$$\Omega'_r \geqslant \omega^*_r(1+\mu_r/\nu_r) > \omega_r(1+\mu_r/\nu_r) > \omega_r. \tag{18}$$

Thus the instability due to internal damping certainly occurs at a speed higher than that for the corresponding symmetrical shaft of flexural rigidity EI in the same bearings.

There remains the instability that is governed by inequality (13), which is independent of the internal damping. Inspection of this condition shows that the shaft may be unstable in the rth pair of modes at speeds of rotation Ω given by

$$(1-2\mu_r^2) - \left[\left(\frac{\omega_r'^2-\omega_r^2}{\omega_r'^2+\omega_r^2}\right)^2 - 4\mu_r^2(1-\mu_r^2)\right]^{\frac{1}{2}} < \left(\frac{\Omega}{\omega_r^*}\right)^2 < (1-2\mu_r^2) + \left[\left(\frac{\omega_r'^2-\omega_r^2}{\omega_r'^2+\omega_r^2}\right)^2 - 4\mu_r^2(1-\mu_r^2)\right]^{\frac{1}{2}}. \tag{19}$$

For small external damping $\mu_r \ll 1$ and $2\mu_r \ll (\omega_r'^2-\omega_r^2)/(\omega_r'^2+\omega_r^2)$ this inequality reduces to the simpler approximate form

$$\omega_r < \Omega < \omega_r'. \tag{20}$$

Clearly the shaft may be unstable in speed regions bounded approximately by the two critical speeds in each pair of modes. This range of instability in the rth pair of modes can, however, be reduced either by increasing the external damping in the system or by decreasing the axial asymmetry. Indeed the unstable speed range vanishes completely if the damping is given approximately by

$$\frac{b_e}{2A\rho\omega_r^*} = \mu_r > \frac{1}{2}\frac{\omega_r'^2-\omega_r^2}{\omega_r'^2+\omega_r^2} = \frac{1}{2}\frac{(EI)'-EI}{(EI)'+EI}. \tag{21}$$

This form of instability, which is due directly to the unequal shaft stiffnesses, does not arise in shafts possessing axial symmetry. For the latter, the inequalities (19) do not define any real ranges of speed. Inspection of expression (21) suggests that, for any given external damping represented by the damping coefficient b_e (which is independent of the modes in question) the shaft is more likely to be stable in the lower pairs of modes rather than the higher ones, since the modal damping coefficient μ_r decreases as the order of the pair of modes in increased.

The necessity of avoiding this type of instability imposes a considerable restriction on the design of large, high speed rotors. It is for this reason that modern alternator rotors have their pole faces slotted in an attempt to reduce inequalities of stiffness (see figure 3). This design restriction is illustrated by the curves in figure 6.

Relation (21) states that, for the shaft to remain stable at speeds between the critical speeds in the rth pair of modes, the damping coefficient in these modes must exceed a certain critical value, $\bar{\mu}_r$, say, such that

$$\mu_r > \bar{\mu}_r = \frac{1}{2}\frac{(EI)'-EI}{(EI)'+EI}. \tag{22}$$

† Note that this condition need only be considered if $\nu_r > \mu_r$.

12   R. E. D. BISHOP AND A. G. PARKINSON

The variation in $\bar{\mu}_r$ with the degree of asymmetry of shaft cross-section is shown in figure 6 for the three cross-sections of figure 7. The degree of asymmetry is expressed in the form of a non-dimensional factor λ which is the ratio of the thickness of the cross-section in the OU direction to that in the OV direction. Thus $\lambda = OA/OB$, as in figure 7. In considering the curves of figure 6 it must be remembered that μ_r is generally less than 0·1 and often very much smaller.
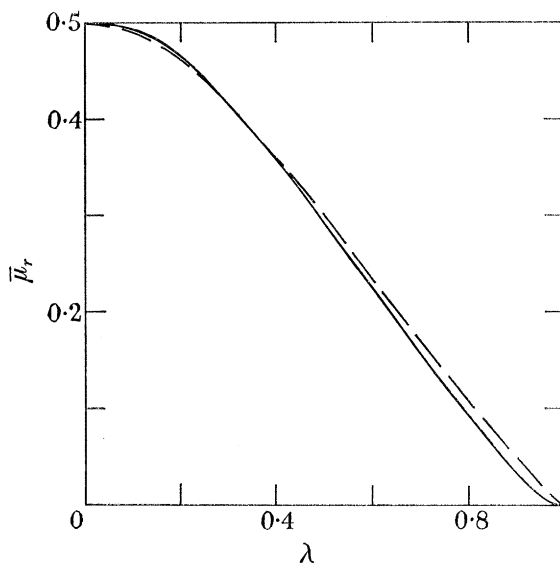

FIGURE 6. ———, Shaft of figure 7 (a); — — — —, shafts of figures 7 (b) and (c).
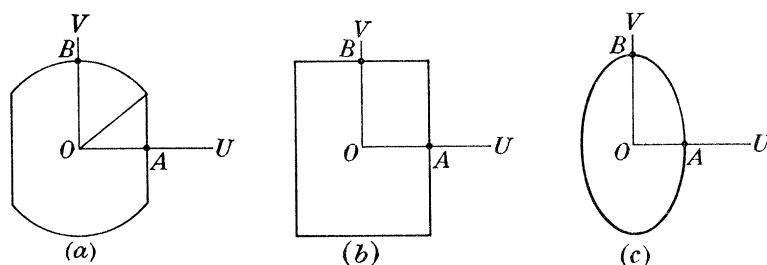

FIGURE 7. (a) Circular shaft with flats parallel to OV; (b) rectangular shaft; (c) elliptical shaft.

(b) *Forced vibration*

The forced vibration of the rotating shaft due to mass unbalance is represented by the particular integral of equation (11) with only the $\bar{a}\Omega^2$ term on the right hand side. This forced vibration may be expressed in the form

$$\eta = \sum_{r=1}^{\infty} \eta_r \phi_r(x)$$

$$= \sum_{r=1}^{\infty} \left[\frac{\bar{a}_r \Omega^2 \, e^{-i\zeta_r} [(\omega_r^{*2} - \Omega^2)^2 + 4\mu_r^2 \omega_r^{*2} \Omega^2]^{\frac{1}{2}} + \frac{1}{2}(\omega_r'^2 - \omega_r^2) \, \bar{a}_r^* \Omega^2}{(\omega_r^2 - \Omega^2)(\omega_r'^2 - \Omega^2) + 4\mu_r^2 \omega_r^{*2} \Omega^2} \right] \phi_r(x), \qquad (23)$$

where $\zeta_r = \tan^{-1} \left(\dfrac{2\mu_r \omega_r^* \Omega}{\omega_r^{*2} - \Omega^2} \right).$ (24)

This expression contains the quantities

$$\left.\begin{aligned} \bar{a}_r &= a_r + \mathrm{i}a'_r, \\ \bar{a}^*_r &= a_r - \mathrm{i}a'_r, \end{aligned}\right\} \tag{25}$$

which are obtained by expanding the mass unbalance in the form of modal components, such that

$$\left.\begin{aligned} \bar{a}(x) &= \sum_{r=1}^{\infty} \bar{a}_r \phi_r(x), \cdot \\ \bar{a}_r &= \frac{1}{Z} \int_0^l \bar{a}(x)\, \phi_r(x)\, \mathrm{d}x. \end{aligned}\right\} \tag{26}$$

The nature of the vibration—or, rather, distortion—described by equation (23) and the associated balancing problem will be discussed in greater detail elsewhere (Parkinson 1965). It will suffice, here, merely to indicate a few of its features. The most obvious characteristic of the distortion defined by relation (23) is that the motion in the rth pair of modes is not in a simple phase relationship with the corresponding component of unbalance, $\bar{a}_r$, as would be the case with an axially symmetric system. At any given speed, the shaft does describe a circular path around the bearing axis (as does a shaft possessing axial symmetry). This is in contrast to the motion of an unbalanced axially symmetric shaft borne in asymmetric bearings (Parkinson 1965). The vibration is, however, independent of the internal damping factor, ν_r. This is a property which the system shares with shafts having axial symmetry (see, for example, Bishop & Gladwell 1959).

Another feature of the result (23) is that the sensitivity of the shaft to a given unbalance depends upon the angular location of the radial planes of unbalance in addition to the distribution of the unbalance along the shaft. This observation can be established as a result of some tedious differentiation of equation (23), but a simpler technique will be adopted here which will also give some physical insight into the problem.

Equation (23) shows that, at a given shaft speed Ω, the distortion in the rth pair of modes may be rewritten in the form

$$\eta_r = [E_r \bar{a}_r \mathrm{e}^{-\mathrm{i}\zeta_r} + F_r \bar{a}^*_r]\,[\text{function of } \Omega], \tag{27}$$

in which E_r is a function of Ω and F_r is a constant. Thus at any particular shaft speed the direction and, in part, the magnitude of this distortion is controlled by the terms inside the first bracket in equation (27). These consist of two factors: (i) a constant vector parallel to $\bar{a}^*_r$ and independent of shaft speed, and (ii) a vector which is speed-dependent and parallel to $\bar{a}_r\,e^{-\mathrm{i}\zeta_r}$.

The combination of these two vectors is illustrated in figure 8 where an angle θ_r has been used, being defined by

$$\tan\theta_r = (a'_r/a_r). \tag{28}$$

That is, θ_r specifies the orientation of the rth modal component of mass unbalance relative to the axes OU, OV. At any particular speed, then, it is clear that the distortion will be a maximum for an unbalance distribution such that these two vectors are in phase. Conversely, when the two vectors are in exact anti-phase the response will be a minimum. Figure 8 shows that (a) the distortion is a maximum if $\theta_r = -(\theta_r - \zeta_r)$, that is if

$$\theta_r = \tfrac{1}{2}\zeta_r = \tfrac{1}{2}\tan^{-1}\left(\frac{2\mu_r \omega^*_r \Omega}{\omega^{*2}_r - \Omega^2}\right), \tag{29}$$

14   R. E. D. BISHOP AND A. G. PARKINSON

and (*b*) the vibration is a minimum if $\theta_r = -(\theta_r - \zeta_r) + \pi$, that is if

$$\theta_r = \theta_r \text{ (for maximum distortion)} + \tfrac{1}{2}\pi. \tag{30}$$

The results (29) and (30) are in agreement with some conclusions of Taylor (1940), who analysed the vibration of a disc on a light, flexible shaft with asymmetric stiffness (see figure 4) and conducted some experiments on a large rotor. Taylor concluded that, at a speed $\Omega = \omega_1^*$,† the maximum and minimum responses are caused by unbalance in radial planes at angles $\theta_1 = \tfrac{1}{4}\pi$ and $\theta_1 = -\tfrac{1}{4}\pi$ respectively, relative to the plane OXU. That is, at this speed, the maximum response is obtained when the plane of unbalance leads the principal plane of minimum stiffness by $\tfrac{1}{4}\pi$ rad and the minimum response is associated with an unbalance plane $\tfrac{1}{4}\pi$ rad behind this plane. There were some discrepancies in Taylor's experimental results—which appear to be displayed also by modern alternator rotors—but one possible source of these may lie in the lack of symmetry that must be associated with plain bearings.
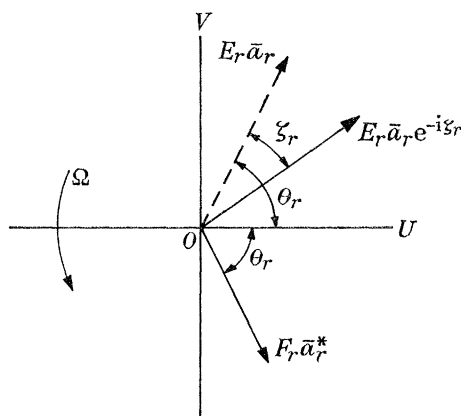

FIGURE 8

The variation of θ_r for maximum distortion is portrayed graphically in figure 9. An alternative presentation, in the form of a polar diagram depicting sensitivity as a function of the angular location of unbalance at $\Omega = \omega_1^*$, is given by Taylor.

For a given unbalance distribution the general nature of the amplitude/speed relationship in the rth pair of modes depends on the inequality of the flexural stiffnesses and on the external damping. Thus for large difference of stiffness, such that inequality (22) is not satisfied, the shaft has infinite amplitudes at each end of the unstable region defined by inequality (19). When the disparity is reduced until equality (22) is satisfied, the pairs of speeds at which an infinite amplitude in the rth pair of modes may occur coalesce at approximately $\Omega = \omega_r^*$. Any further reduction in asymmetry, or increase in external damping, such that inequality (22) is valid, removes the infinite resonance peaks entirely. In these circumstances the amplitude in the rth pair of modes increases to a finite peak at a shaft speed which, for a given shaft, depends on the angle θ_r. The amplitude/speed curve in the rth pair of modes is similar to that for the system of figure 4, which was illustrated by Taylor (1940, figure 7).

† The analysis was confined to a simple two-degree-of-freedom model with a concentrated load and observations were only made in the neighbourhood of the first critical speed ω_1^*. Taylor's results relate essentially to the motion in the first pair of modes, being based on the rudimentary Jeffcott model of a rotating shaft.

For all inequalities of stiffness and for all external damping, the variation of the phase angle ζ_r is identical to that for a symmetrical shaft with a critical speed ω_r^* in the rth pair of modes.
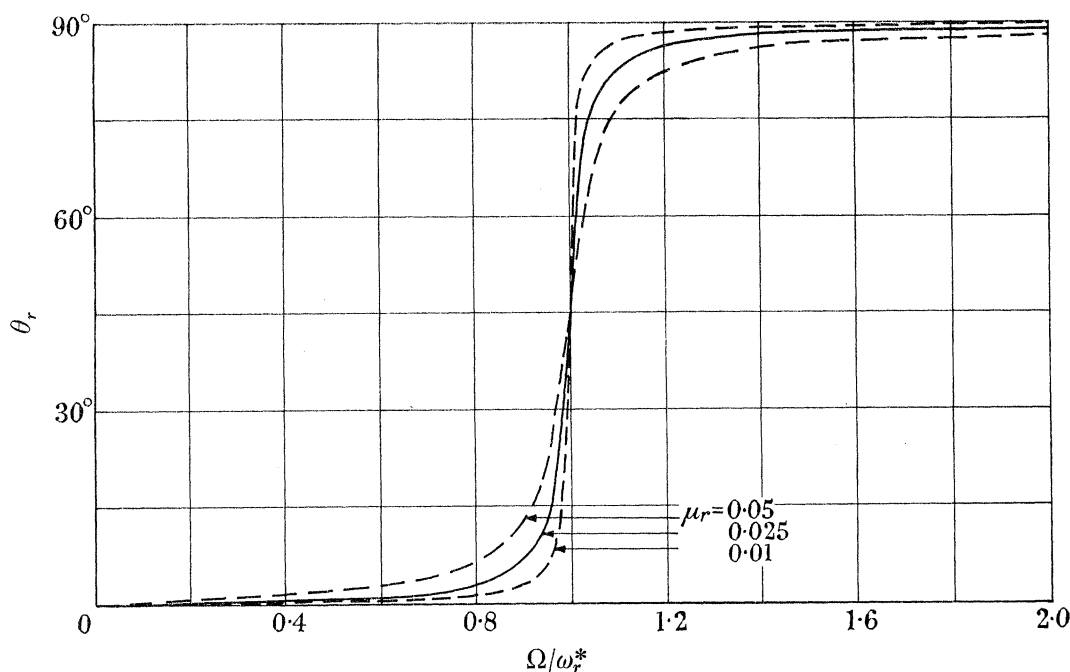

FIGURE 9

VIBRATION OF A UNIFORM, HORIZONTAL SHAFT DUE TO ITS OWN WEIGHT

So far, we have referred to the free vibration and the forced vibration due to mass unbalance of a rotating, asymmetric shaft. These vibrations may be executed whether the shaft is rotating about a vertical or a horizontal axis. Indeed, if the shaft is supported vertically then the entire motion is confined to these forms of vibration. But if the shaft rotates about a horizontal axis (as is usual) the equations of motion (8) and (9) must be used with the terms on the right hand side which represent the weight of the shaft. It is the purpose of this section—and indeed the main purpose of this paper—to investigate the distortion of the shaft due to the weight force.

The relevant equations of motion are now

$$\ddot{v} + \left[\frac{b_e + b_i}{A\rho}\right]\dot{v} - \Omega^2 v + \frac{EI}{A\rho}\frac{\partial^4 v}{\partial x^4} - 2\Omega\dot{v}' - \frac{b_e}{A\rho}\Omega v' = -g\sin\Omega t, \tag{31}$$

$$\ddot{v}' + \left[\frac{b_e + b_i}{A\rho}\right]\dot{v}' - \Omega^2 v' + \frac{(EI)'}{A\rho}\frac{\partial^4 v'}{\partial x^4} + 2\Omega\dot{v} + \frac{b_e}{A\rho}\Omega v = -g\cos\Omega t. \tag{32}$$

Alternatively these equations can be replaced by the single complex equation

$$\ddot{\eta} + \left[\frac{b_e + b_i}{A\rho}\right]\dot{\eta} - \Omega^2\eta + \frac{1}{2}\left[\frac{EI + (EI)'}{A\rho}\right]\frac{\partial^4\eta}{\partial x^4}$$

$$+ \frac{1}{2}\left[\frac{EI - (EI)'}{A\rho}\right]\frac{\partial^4\eta^*}{\partial x^4} + 2i\Omega\dot{\eta} + i\frac{b_e}{A\rho}\Omega\eta = -ig\,e^{-i\Omega t}. \tag{33}$$

The general solution for the forced motion governed by equations (31) and (32) that satisfies the boundary conditions at each end of the shaft may be written in the following form:

$$
\begin{aligned}
v &= \sum_{r=1}^{\infty} (A_r \sin \Omega t + B_r \cos \Omega t)\, \phi_r(x), \\
v' &= \sum_{r=1}^{\infty} (C_r \sin \Omega t + D_r \cos \Omega t)\, \phi_r(x).
\end{aligned}
\tag{34}
$$

If these expressions are substituted into equations (31) and (32) and the motion separated into modal components by using the orthogonality condition (7), then the motion in the rth pair of modes is described by the following matrix equation

$$
\begin{bmatrix}
\omega_r^2 - 2\Omega^2 & -2(\mu_r + \nu_r)\,\Omega\omega_r^* & -2\mu_r\,\omega_r^*\Omega & 2\Omega^2 \\
2(\mu_r + \nu_r)\,\Omega\omega_r^* & \omega_r^2 - 2\Omega^2 & -2\Omega^2 & -2\mu_r\,\omega_r^*\Omega \\
2\mu_r\,\omega_r^*\Omega & -2\Omega^2 & \omega_r'^2 - 2\Omega^2 & -2(\mu_r + \nu_r)\,\Omega\omega_r^* \\
2\Omega^2 & 2\mu_r\,\omega_r^*\Omega & 2(\mu_r + \nu_r)\,\omega_r^*\Omega & \omega_r'^2 - 2\Omega^2
\end{bmatrix}
\begin{bmatrix} A_r \\ B_r \\ C_r \\ D_r \end{bmatrix}
=
\begin{bmatrix} -g_r \\ 0 \\ 0 \\ -g_r \end{bmatrix},
\tag{35}
$$

where

$$
g_r = \frac{1}{Z} \int_0^l g \phi_r(x)\, \mathrm{d}x = \frac{g}{Z} \int_0^l \phi_r(x)\, \mathrm{d}x.
\tag{36}
$$

The solution of equation (35) for the four coefficients A_r, B_r, C_r and D_r is lengthy and the resulting expressions are complicated. Later on, we shall take up a simplified special case, but it is worthwhile, before doing so, to examine the nature of the solution (34). This solution may be expressed in the complex form

$$
\eta = \sum_{r=1}^{\infty} (P_r\, \mathrm{e}^{\mathrm{i}\Omega t} + Q_r\, \mathrm{e}^{-\mathrm{i}\Omega t})\, \phi_r(x),
\tag{37}
$$

where the coefficients P_r and Q_r are complex. In general, then, the weight of the shaft causes a motion in each pair of modes that would be seen by an observer rotating with the shaft as the sum of forward and backward circular motions—both executed with the speed Ω.

It is perhaps more useful to note the form of the motion (37) in space—that is, relative to the fixed axes, OYZ. In complex notation, the displacement is

$$
u + \mathrm{i}u' = \xi = \sum_{r=1}^{\infty} \xi_r \phi_r(x).
\tag{38}
$$

This is related to the displacement η through equations (1), the transformation in complex notation being

$$
\xi = \eta\, \mathrm{e}^{\mathrm{i}\Omega t}.
\tag{39}
$$

The vibration (37) can thus be expressed in the form

$$
\xi = \sum_{r=1}^{\infty} (P_r\, \mathrm{e}^{\mathrm{i}2\Omega t} + Q_r)\, \phi_r(x).
\tag{40}
$$

This describes the motion, as it is seen by a stationary observer.

So far as the rth pair of modes is concerned, then, the shaft weight causes:

(i) a steady deflexion $Q_r\phi_r(x)$ which is in the nature of a 'sag' (though it will not, in general, be vertically downwards) together with

(ii) a forward rotation with *twice* the angular velocity of the shaft rotation.

It is of interest to notice certain special cases. If there is no difference between EI and $(EI)'$, so that $\omega_r = \omega_r'$, the square matrix in equation (35) may be partitioned in a simple fashion. When this condition obtains, it may be shown that

$$P_r = 0; \quad Q_r = \frac{-\mathrm{i}g_r}{\omega_r^2 - 2\mathrm{i}\nu_r\,\omega_r\,\Omega}. \tag{41}$$

That is to say, the 'double-frequency' vibration does not occur, and the static sag becomes that of a shaft with axial symmetry (Bishop & Gladwell 1959).

A second special case will be examined in the next section. It is that of a shaft which, while it possesses unequal flexibilities, has no internal damping. The assumption that $\nu_r = 0$ leads to considerable simplification of the theory without—it seems—making it too restricted. It might be added that few writers have made allowance for internal damping when studying *any* aspect of shaft vibration, let alone the present problem. Two prominent exceptions to this are Smith (1933) and Dimentberg (1961), who both discuss some of the effects of internal damping.

Shaft with no internal damping

If a large alternator rotor is slung from a crane and made to execute a forced vibration in the horizontal plane as a free–free beam, it is found that very little power is needed. Modal Q factors of 200 to 400 have been reported by P. G. Morton in a contribution to the discussion of the paper by Lindley & Bishop (1963). This observation has also been made by L. S. Moore of G.E.C. (Witton). By contrast, the modal Q-factors of such shafts when they are rotating are relatively low, being about 6 (see Lindley & Bishop 1963). Although these results are by no means based on refined experiment or theory, they do give a clear indication that $\mu_r \gg \nu_r$ for large alternators. We now proceed, therefore, under the simplifying assumption that $\nu_r = 0$.

If the square matrix of equation (35) is now inverted it gives

$$A_r = \frac{[(\omega_r'^2 - 4\Omega^2)(4\omega_r^{*2}\Omega^2 - \omega_r^2\omega_r'^2) - 16\mu_r^2\omega_r^{*4}\Omega^2]\,g_r}{\Delta},$$

$$B_r = \frac{2\mu_r\omega_r^*\omega_r'^2\,\Omega(\omega_r'^2 - \omega_r^2)\,g_r}{\Delta},$$

$$C_r = \frac{2\mu_r\omega_r^*\omega_r^2\,\Omega(\omega_r'^2 - \omega_r^2)\,g_r}{\Delta}, \tag{42}$$

$$D_r = \frac{[(4\omega_r^{*2}\Omega^2 - \omega_r^2\omega_r'^2)(\omega_r^2 - 4\Omega^2) - 16\mu_r^2\omega_r^{*4}\Omega^2]\,g_r}{\Delta},$$

where
$$\Delta = (4\omega_r^{*2}\Omega^2 - \omega_r^2\omega_r'^2)^2 + 16\mu_r^2\omega_r^{*6}\Omega^2.$$

The additional complexity of allowing for internal damping may be illustrated by the expression for Δ obtained from the complete solution of equation (35). We find that

$$\Delta = (\omega_r^2\omega_r'^2 - 4\omega_r^{*2}\Omega^2)^2 + 8\omega_r^{*2}\Omega^2[8\nu_r^2\Omega^4 + 2\nu_r^2\{(2\mu_r + \nu_r)^2 - 2\}\omega_r^{*2}\Omega^2$$
$$+ 2(\mu_r + \nu_r)^2\,\omega_r^{*4} - \nu_r(2\mu_r + \nu_r)\,\omega_r^2\omega_r'^2]. \tag{43}$$

When they are substituted into expressions (34), the results (42) give the information necessary for finding P_r and Q_r in equations (37) and (40). It is found, in fact, that

$$P_r = \frac{\mathrm{i}g_r(\omega_r'^2 - \omega_r^2)\,\mathrm{e}^{-\mathrm{i}\sigma_r}}{8\omega_r^{*2}\,\sqrt{[(\Omega_r^2 - \Omega^2)^2 + \mu_r^2\,\omega_r^{*2}\Omega^2]}},\tag{44}$$

$$Q_r = \frac{g_r[\mu_r\omega_r^*\Omega(\omega_r'^2 - \omega_r^2)^2 + \mathrm{i}4\omega_r^{*2}\{(\Omega^2 - \Omega_r^2)\,(\omega_r^{*2} - 4\Omega^2) - 4\mu_r^2\,\omega_r^{*2}\Omega^2\}]}{16\omega_r^{*4}[(\Omega_r^2 - \Omega^2)^2 + \mu_r^2\,\omega_r^{*2}\Omega^2]},\tag{45}$$

where

$$\Omega_r = \frac{\omega_r\,\omega_r'}{2\omega_r^*}\tag{46}$$

and

$$\sigma_r = \tan^{-1}\left(\frac{\mu_r\omega_r^*\,\Omega}{\Omega_r^2 - \Omega^2}\right).\tag{47}$$

The symbol Ω_r introduced in equation (46) turns out to be of physical significance, being of the nature of a 'critical speed'. By rearranging equation (46) it is found that

$$\Omega_r = \tfrac{1}{2}\omega_r^*\,\sqrt{\left[1 - \left(\frac{\omega_r'^2 - \omega_r^2}{\omega_r'^2 + \omega_r^2}\right)^2\right]},\tag{48}$$

and, for shafts with only small inequality of stiffness (such as large alternator rotors), this quantity has the approximate value

$$\Omega_r \doteqdot \tfrac{1}{2}\omega_r^*.\tag{49}$$

It has been shown that the distortion of the horizontal shaft, due to its own weight, can be separated into two distinct parts by writing

$$\xi = \xi^{(1)} + \xi^{(2)},\tag{50}$$

where

$$\xi^{(1)} = \sum_{r=1}^{\infty} \xi_r^{(1)}\phi_r(x) = \sum_{r=1}^{\infty} Q_r\phi_r(x)\tag{51}$$

and

$$\xi^{(2)} = \sum_{r=1}^{\infty} \xi_r^{(2)}\phi_r(x) = \sum_{r=1}^{\infty} P_r\phi_r(x)\,\mathrm{e}^{2\mathrm{i}\Omega t}.\tag{52}$$

At any speed Ω the shaft has a constant deflexion described by relation (51). The centre line of the shaft also rotates about the axis of the bearings with a speed 2Ω, while the shaft rotates about its own axis with a speed Ω. That is, the shaft axis performs a second order vibration relative to the fixed axes $OXYZ$. We will discuss the two components of the total vibration separately.

(a) Constant deflexion

At low speeds Ω the constant deflexion in the rth pair of modes is given by

$$\xi_r^{(1)} \to -\mathrm{i}g_r/4\Omega_r^2 \quad (\Omega \ll \Omega_r).\tag{53}$$

As one would expect, the constant deflexion is vertically downwards (the axis OZ is defined to be vertically upwards).

If the speed of rotation Ω is increased, the denominator of equation (45) suggests that a sort of resonance should occur in the rth pair of modes at the speed Ω_r (see equations (48) and (49))—a possibility which obviously must be examined. In fact at this speed the constant deflexion has the form

$$\xi_r^{(1)} = \frac{g_r}{\omega_r^*}\left[\frac{1}{4\Omega_r\mu_r}\left(\frac{\omega_r'^2 - \omega_r^2}{\omega_r'^2 + \omega_r^2}\right)^2 - \frac{\mathrm{i}}{\omega_r^*}\right] \quad (\Omega = \Omega_r).\tag{54}$$

Thus, when the shaft has a speed Ω_r the constant deflexion has components in the vertical and horizontal directions. Since $\Omega_r \doteqdot \frac{1}{2}\omega_r^*$, normally, the constant deflexion in the vertical direction is virtually unchanged from its magnitude at low speeds. Moreover, the horizontal deflexion represented by the real part of equation (54) is small. In practice one is interested mainly in shafts with small asymmetry and which are stable in the intervals defined by the pairs of speeds (20). For these shafts the asymmetry must be sufficiently small to satisfy inequality (21). With normal external damping this implies that the magnitude of the imaginary part of $\xi_r^{(1)}$ in equation (54) is considerably greater than that of the real part. The ratio of the horizontal deflexion to the vertical deflexion in these circumstances is less than $\mu_r \omega_r^*/\Omega_r$. Therefore the constant displacement of the shaft at a speed Ω_r is still predominantly vertically downwards and of approximately the same magnitude as the deflexion at low speed. There is no danger of a large increase in this displacement at the speed Ω_r and no true resonance in the constant deflexion.

Further increase in shaft speed to values well above Ω_r produces a constant displacement of the form

$$\xi_r^{(1)} \to -\mathrm{i}g_r/\omega_r^{*2} \quad (\Omega \gg \Omega_r). \tag{55}$$

That is, at high speeds the constant deflexion in the rth pair of modes is again vertical, and approximately equal to the displacement at low speed. The assumption that $\nu_r = 0$ is not made in a previous treatment of shafts possessing axial symmetry (Bishop & Gladwell 1959). The results indicate that the present conclusions may be modified slightly by the presence of internal damping. Clearly the constant deflexion does not vary appreciably with shaft speed.

(b) Second order vibration

The second order (or 'twice-per-revolution') component of the vibration described by equation (40) is of the form

$$\xi^{(2)} = \sum_{r=1}^{\infty} \xi_r^{(2)}\phi_r(x) = \sum_{r=1}^{\infty} \frac{\overline{A}_r\,\mathrm{e}^{-\mathrm{i}\sigma_r}\phi_r(x)}{\sqrt{[(\Omega_r^2-\Omega^2)^2 + \mu_r^2\omega_r^{*2}\Omega^2]}}\,\mathrm{e}^{2\mathrm{i}\Omega t}, \tag{56}$$

where

$$\overline{A}_r = \frac{\mathrm{i}g_r}{4}\left(\frac{\omega_r'^2 - \omega_r^2}{\omega_r'^2 + \omega_r^2}\right). \tag{57}$$

If the disparity between stiffnesses is modest, so that equation (49) holds good, this vibration is described approximately by

$$\xi^{(2)} \doteqdot \sum_{r=1}^{\infty} \frac{\overline{A}_r\,\mathrm{e}^{-\mathrm{i}\sigma_r}\phi_r(x)}{\sqrt{[(\Omega_r^2-\Omega^2)^2 + 4\mu_r^2\Omega_r^2\Omega^2]}}\,\mathrm{e}^{2\mathrm{i}\Omega t}, \tag{58}$$

where

$$\sigma_r = \tan^{-1}\left(\frac{2\mu_r\Omega_r\Omega}{\Omega_r^2-\Omega^2}\right), \tag{59}$$

and where the effectiveness of g_r in producing an 'amplitude of excitation', $\overline{A}_r$, is fairly small.

The expressions (47) and (56) or (58) and (59) are similar to those representing the forced vibration in the rth mode due to mass unbalance of a shaft with axial symmetry in the same bearings. For the symmetrical shaft, $\omega_r' = \omega_r = \omega_r^*$ and it is shown elsewhere (Bishop & Gladwell 1959) that the rth component of mass unbalance $\overline{a}_r = a_r + \mathrm{i}a_r'$ produces a vibration

$$\xi = \sum_{r=1}^{\infty} \frac{\Omega^2\overline{a}_r\,\mathrm{e}^{-\mathrm{i}\zeta_r}\phi_r(x)}{\sqrt{[(\omega_r^{*2}-\Omega^2)^2 + 4\mu_r^2\omega_r^{*2}\Omega^2]}}\,\mathrm{e}^{\mathrm{i}\Omega t}, \tag{60}$$

where

$$\zeta_r = \tan^{-1}\left(\frac{2\mu_r\omega_r^*\Omega}{\omega_r^{*2}-\Omega^2}\right). \tag{61}$$

The frequency of the vibrations represented by expressions (56) and (58) on the one hand and by (60) on the other are not the same, but the other factors are similar. The second order vibration of equations (56) or (58) is, therefore, a forced vibration with critical speeds $\Omega_1, \Omega_2, \Omega_3, \ldots$. For any shaft speed Ω the centre E of the shaft at any axial section describes a circle about the bearing axis with a speed 2Ω.

In so far as the magnitude of the component of the exciting force in the rth pair of modes (represented by $\overline{A}_r$) is independent of shaft speed Ω, the second order vibration is even more closely analogous to the forced vibration due to elastic unbalance—or initial lack of straightness—of an axially symmetric shaft. Thus equation (90) of Bishop (1959) gives the expression

$$\xi = \sum_{r=1}^{\infty} \frac{\omega_r^{*2} \overline{\epsilon}_r \, e^{-i\zeta_r} \phi_r(x)}{\sqrt{[(\omega_r^{*2} - \Omega^2)^2 + 4\mu_r^2 \omega_r^{*2} \Omega^2]}} \, e^{i\Omega t} \tag{62}$$

for this motion, where the initial bend is represented by

$$v_0 + iv_0' = \sum_{r=1}^{\infty} \overline{\epsilon}_r \, \phi_r(x). \tag{63}$$

Parts of the descriptions given previously of these two forms of first order vibration are directly applicable to the present second order motion (for example, Parkinson, Jackson & Bishop 1963). Thus at low speeds the distortion in the rth pair of modes becomes

$$\xi_r^{(2)} \to \frac{\overline{A}_r \, e^{2i\Omega t}}{\Omega_r^2} = \frac{i g_r}{4\Omega_r^2} \left(\frac{\omega_r'^2 - \omega_r^2}{\omega_r'^2 + \omega_r^2} \right) e^{2i\Omega t} \quad (\Omega \ll \Omega_r). \tag{64}$$

At these low speeds of shaft rotation the distortion of the shaft in the rth pair of modes is in phase with the modal component of the exciting force $\overline{A}_r \, e^{2i\Omega t}$. Comparison of equations (53) and (64) shows that, at low speeds Ω, the amplitude of the twice-per-revolution vibration is less than the constant deflexion $\xi_r^{(1)}$.

The circular motion $\xi_r^{(2)}$ of the centre E of any cross-section of the shaft while the shaft is rotating through half a revolution about its own axis is illustrated in figure 10 (a) (i). The second half revolution produces a similar motion of the centre E and is sketched in figure 10 (a) (ii). The arrow should be thought of as being marked on the cross-section so as to pass through E in figure 5 and lie parallel to the OV axis. At these very low speeds, inertia forces play no significant part and the vibration can be thought of in terms of statics; thus the sag is greatest when the plane of maximum flexural rigidity is horizontal.

As the speed Ω of rotation of the shaft is increased the amplitude of the twice-per-revolution vibration increases. The shaft approaches a state of resonance as $\Omega \to \Omega_r$, at which speed the vibration in the rth pair of modes becomes

$$\xi_r^{(2)} = \frac{\overline{A}_r \, e^{-i\pi/2} \, e^{2i\Omega t}}{\mu_r \omega_r^* \Omega_r} = \frac{g_r}{4\mu_r \omega_r^* \Omega_r} \left(\frac{\omega_r'^2 - \omega_r^2}{\omega_r'^2 + \omega_r^2} \right) e^{2i\Omega t}$$

$$= \frac{g_r}{\Omega_r} \left(\frac{A\rho}{2b_e} \right) \frac{(EI)' - EI}{(EI)' + EI} e^{2i\Omega t} \quad (\Omega = \Omega_r). \tag{65}$$

The amplitude of this vibration is considerably larger than that at low speeds, being roughly $1/2\mu_r$ times as great. The response in the rth pair of modes is $\frac{1}{2}\pi$ in phase behind the corresponding component of the exciting force, $\overline{A}_r \, e^{2i\Omega t}$. The actual circular motion of a point on the shaft centre line is illustrated in figures 10 (b) (i) and 10 (b) (ii) for one complete rotation

of the shaft about its own axis. The presence of the term Ω_r in the last expression for $\xi_r^{(2)}$ in equation (65) shows that, ignoring the factor g_r which is discussed later, the modal components decrease in magnitude, as the order of the mode increases.
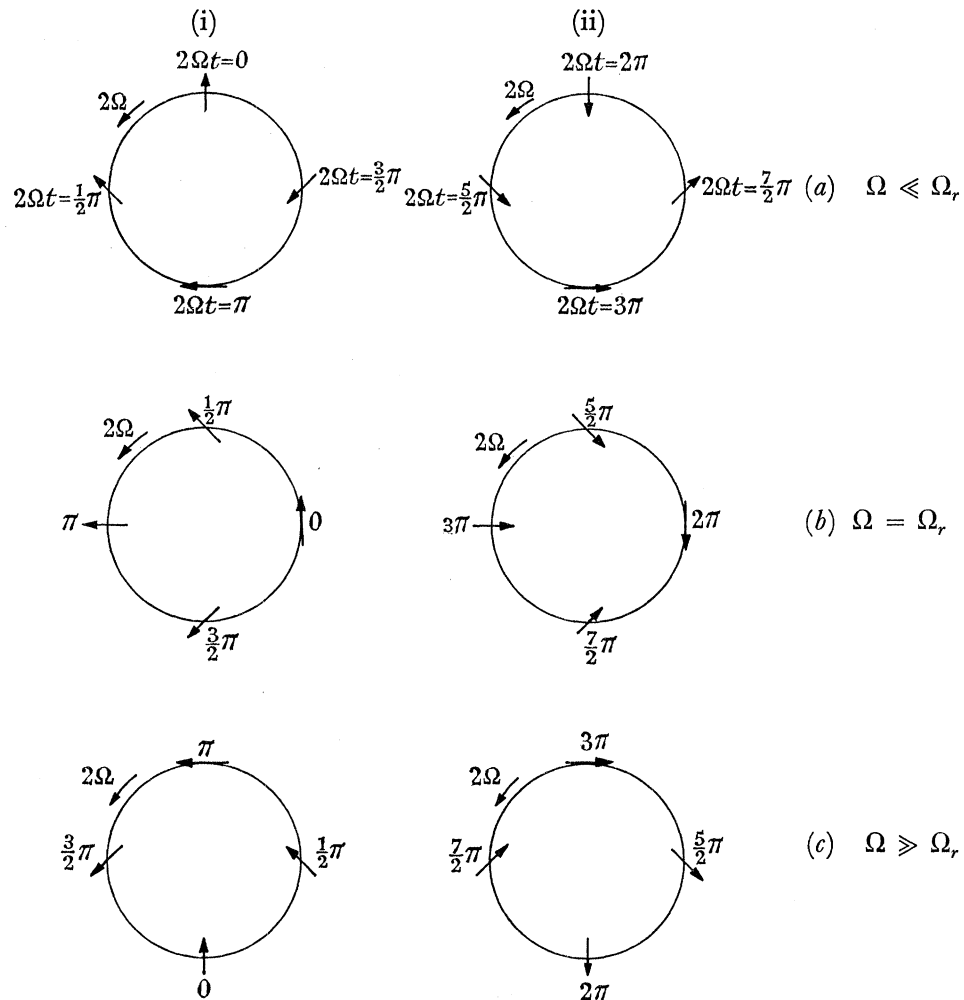

FIGURE 10

It should be noted that for shafts which are stable at all speeds between $\Omega = \omega_r$ and ω_r'—that is, for which the external damping factor satisfies inequality (21)—the amplitude of the displacement $\xi_r^{(2)}$ of equation (65) is subject to the limitation

$$|\xi_r^{(2)}| < \frac{g_r}{2\omega_r^* \Omega_r} \doteqdot \frac{g_r}{4\Omega_r^2} \doteqdot \frac{g_r}{\omega_r^{*2}}.$$

If this result is compared with that of equation (53) it shows that, even when the second order vibration has its maximum amplitude, this is not greater than the approximately constant, non-rotating deflexion of equations (53), (54) and (55). It is worth remarking that, normally, static sag is not monitored for alternator shafts at speed. Indeed, commonly even the measured vibration is not that of the shaft, but of the bearing housings. These theoretical predictions seem to throw emphasis on the need to measure sag and its variation with speed.

Finally, for very high shaft speeds, the twice-per-revolution vibration in the rth pair of modes has the form

$$\zeta_r^{(2)} \to \frac{\bar{A}_r \, e^{-i\pi} \, e^{2i\Omega t}}{\Omega^2} = -\frac{ig_r}{4\Omega^2} \left(\frac{\omega_r'^2 - \omega_r^2}{\omega_r'^2 + \omega_r^2}\right) e^{2i\Omega t} \quad (\Omega \gg \Omega_r). \tag{67}$$

This distortion is very small and is approximately in antiphase with the exciting force component $\bar{A}_r e^{2i\Omega t}$. The double circular motion of the shaft centre during one revolution of the shaft about its own axis through E is illustrated in figures 10 (c) (i) and 10 (c) (ii).

It is of interest to note that Hull (1961) published experimental results for a rotor consisting of a disc supported on the end of a light cantilever shaft which are in agreement with the predictions of figures 10 (a) and (c).
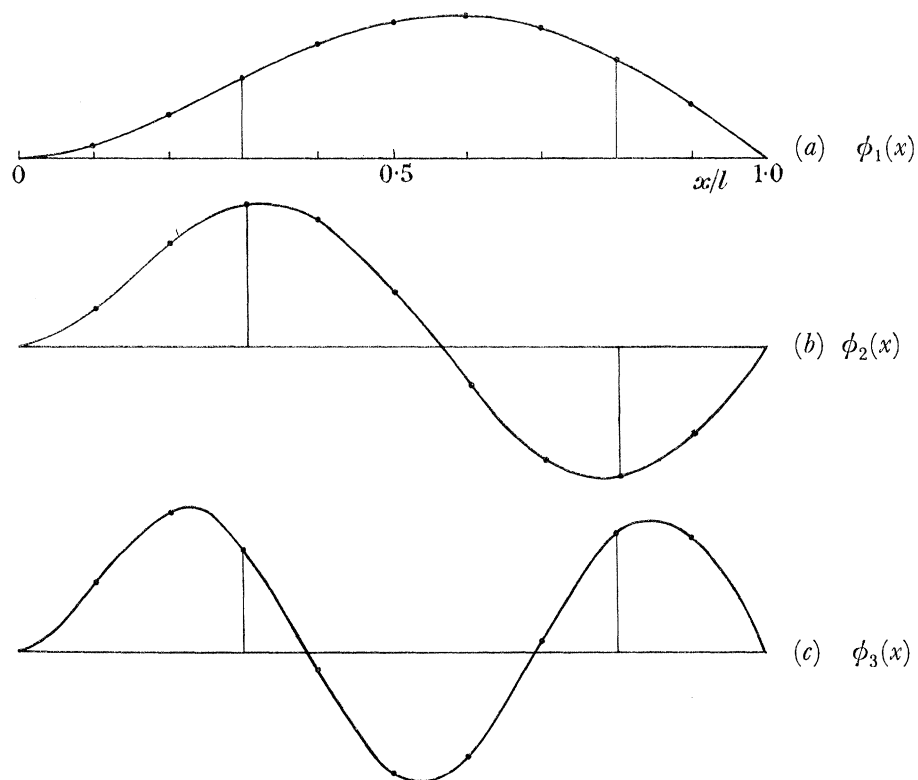

FIGURE 11

It has been shown that the weight of a uniform horizontal rotating shaft with dual stiffness can generate two forms of vibration—a non-rotating displacement and a second order deflexion. These vibrations are not entirely a consequence of the inequality of stiffness, however. For an axially symmetric shaft the non-rotating component of the deflexion described by equation (51) still occurs, although in a modified form. It is given by equations (40) and (41), although for the purposes of comparison here it is necessary to set $\nu_r = 0$. The second order part of the vibration, however, is created completely by the inequality of shaft stiffness (see equations (44) and (52)). The motion is, moreover, independent of mass or elastic unbalance. If, therefore, the twice-per-revolution vibration is larger than is desirable for any particular shaft, it can only be reduced by decreasing the disparity of stiffness—that is by modifying the design of the shaft.

The seriousness of the second order vibration varies from mode to mode. The component g_r of the disturbing force in the rth pair of modes is related to the corresponding characteristic function $\phi_r(x)$ by equation (36). Intuition suggests that the component g_1, for the first pair of modes, is greater than all other components. The characteristic functions for a uniform 'clamped-pinned' shaft are sketched in figure 11. Clearly the area under the curve representing $\phi_1(x)$ in figure 11 (*a*) is greater than the net areas under the curves for $\phi_2(x)$ and $\phi_3(x)$ (shown in figures 11 (*b*) and (*c*)). Thus g_1 is greater than g_2 or g_3 for this shaft.

The areas under the curves for the even numbered functions $\phi_2, \phi_4, \ldots,$ all vanish if the shaft concerned is symmetrical about its mid-span section. In this event, the even numbered components are all zero. In practice, many shafts are at least approximately symmetrical about mid-span so that one would expect the even modal components to be small.

Mortensen & Ryan (1940) reported a test on a simple model of a two-pole alternator rotor for which a second order vibration was observed with a critical speed at $\frac{1}{2}\omega_1^*$. There was, however, no similar resonance in the second pair of modes with a critical speed of $\frac{1}{2}\omega_2^*$.

This matter of the relative magnitudes of the modal components is of some technical importance. A table of values is therefore presented in the Appendix. The table lists the modal components g_r of the weight force in the first five pairs of modes for all uniform shafts with ideal end conditions.

ISOLATION OF MODES IN SECOND ORDER VIBRATION

In recent work on shafts possessing axial symmetry, a technique much used in resonance testing has been adapted to the problem of separating the forced vibration into modal components. Examples of this forced vibration are contained in equations (60) and (62). Initially this research was concerned with shafts with close natural frequencies in flexure. Adjacent modes of such shafts can interact and the application of a modal balancing process— which depends on treating each mode individually—can thereby be made difficult. When a suitable means of isolating the modes had been found, however, the simplicity of the method suggested that it might be a valuable tool in the interpretation of observations of the forced vibration even when the critical speeds are widely spaced apart. This work has been fully discussed elsewhere (Bishop & Parkinson 1963). The purpose of the present section is to demonstrate that the same technique can be used with advantage in analysing experimental data on the second order vibration of a horizontal shaft with unequal stiffnesses.

In essence the method consists of plotting the complex response vector η on an Argand diagram. It is found that the end of the response vector in any mode very nearly describes a circle. For example the rth component of the response of an axially symmetric shaft to mass unbalance is given by

$$\eta_r = \frac{e^{-i\zeta_r}}{\sqrt{[(\omega_r^{*2}-\Omega^2)^2+4\mu_r^2\,\omega_r^{*2}\Omega^2]}}\,\Omega^2\bar{a}_r \tag{68}$$

(see equations (60) and (61)). The response vector **OP** is plotted on an Argand diagram in figure 12. The real axis OR is now defined as being parallel to the force vector of excitation in the rth pair of modes and the imaginary axis is located as shown. The figure shows the response of the shaft relative to the direction of the modal component of the force. If the whole figure is imagined as rotating counterclockwise with angular velocity Ω, then the

line **OP** gives the response ξ through the conventional rotating-line representation of a harmonically varying quantity.

The nearly circular locus has two important properties. First, the point D on the circle which corresponds to the critical speed, $\Omega = \omega_r$, is the point at which the rate of change of frequency with distance along the circular arc is a minimum. That is, if the response is plotted at equal intervals in shaft speed, D is the point with maximum spacing of points along the arc. This is illustrated roughly by the spacing of the points in figure 12. Secondly,
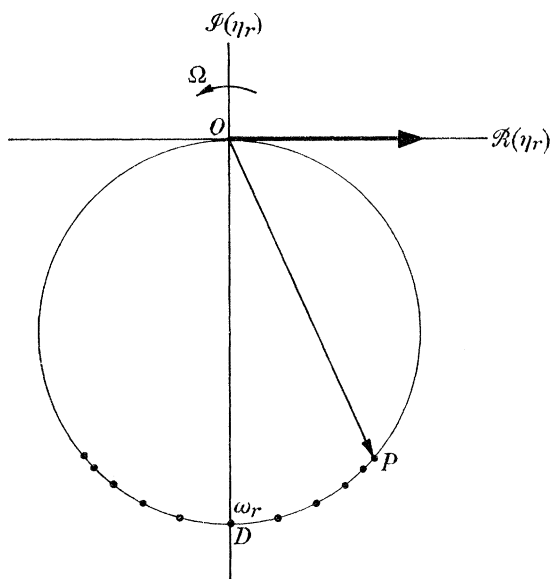
FIGURE 12

the diameter OD (or 'resonance diameter') of the modal response circle is perpendicular to the real axis—that is to the direction of the line representing the exciting force. This is because there is a phase lag of $\frac{1}{2}\pi$ rad in the condition of resonance. Either of these properties can be used to determine the critical speed and the plane of unbalance in the rth pair of modes (see Bishop & Parkinson 1963). The modal circle can also provide the value of the external damping coefficient μ_r in the rth pair of modes (for example, see Bishop & Gladwell 1963).

If the total response vector (see equation (60)) is plotted in this manner for a wide range of speeds, including several critical values, the response locus consists of a combination of the corresponding modal circular arcs. These circles do not, in general, pass through the origin O. For near resonance in any one mode, the total displacement vector may also contain a nearly constant contribution from the other (extraneous) modes. As a consequence the corresponding modal circle is displaced from the origin by this constant vector.

Furthermore, equation (60) shows that the direction of the exciting force in each mode depends on the direction of the component of unbalance, $\bar{a}_r$. In plotting the complete displacement vector, η, an arbitrary datum line must be assigned to be the real axis in the Argand diagram. The forces in the various modes have differing directions relative to this datum line. Consequently the resonance diameter, OD, may have a different direction for each mode. As an example, we reproduce in figure 13 the locus of the response vector for

a uniform continuous shaft in a speed range including the two lowest critical speeds (see Bishop & Parkinson 1963, figure 20 (a)).

The similarity between the second order vibration described by equations (56) and (57) on the one hand and the forced vibration of an axially symmetric shaft represented by expression (60) on the other has been noted earlier in this paper. One outcome of this similarity is that the graphical analysis outlined above can be applied to the second order vibration. Indeed in one respect the twice-per-revolution vibration is simpler to portray in this way than the distortion of an axially symmetric shaft due to mass unbalance. The reason for this may be seen from the following argument.
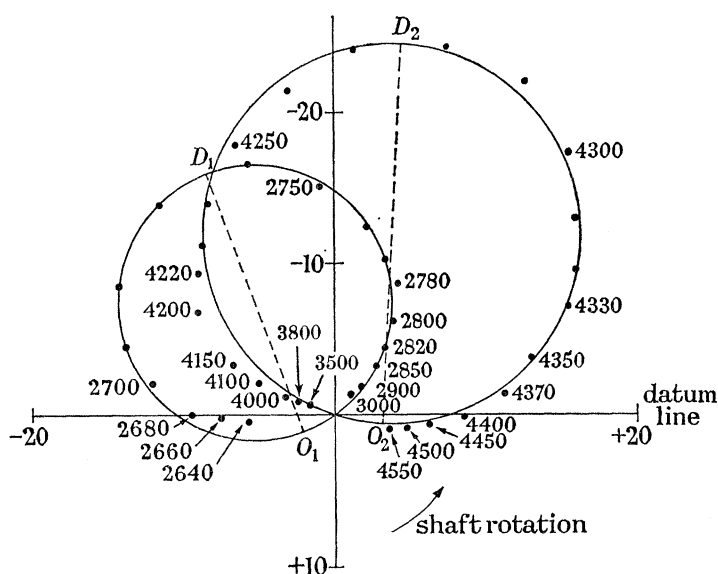

Figure 13. The axes are graduated in multiples of 0·001 in., the speeds of observation being marked in rev/min and at intervals of 10 rev/min in the region of the critical speeds. The resonance diameters in the first and second modes are indicated by the lines O_1D_1 and O_2D_2 respectively.

Equation (58) gives

$$\xi_r^{(2)} \doteq \left\{ \frac{\overline{A}_r \, e^{-i\sigma_r}}{\sqrt{[(\Omega_r^2 - \Omega^2)^2 + 4\mu_r^2 \Omega_r^2 \Omega^2]}} \right\} e^{2i\Omega t} \qquad (69)$$

for the rth pair of modes when the difference between the stiffnesses is fairly small. Here

$$\left. \begin{aligned} \overline{A}_r &= \tfrac{1}{4}ig_r \left(\frac{\omega_r'^2 - \omega_r^2}{\omega_r'^2 + \omega_r^2} \right) = \text{imaginary constant,} \\ \sigma_r &= \tan^{-1} \left(\frac{2\mu_r \Omega_r \Omega}{\Omega_r^2 - \Omega^2} \right), \\ \Omega_r &\doteq \tfrac{1}{2}\omega_r^*. \end{aligned} \right\} \qquad (70)$$

The contents of the curly brackets in equation (69) depend on Ω in the same was as η_r does in equation (68). In other words they will produce a circle diagram of the same type when plotted for different values of Ω.

According to equation (69) the centre of the shaft executes a circular motion of the form

$$\xi_r^{(2)} = R_r \exp \{ i[2\Omega t + \tfrac{1}{2}\pi - \sigma_r] \}, \qquad (71)$$

where R_r is the radius of the circle. The real and imaginary parts of $\xi_r^{(2)}$ are the double-frequency contributions to the displacements u in the direction OY and u' in the direction OZ respectively (see figure 5). This physical interpretation shows how the circle diagram may be plotted in practice. For the radius R_r may be found (to within a multiplying scale factor) by monitoring one of the components of displacement, u say, and filtering it at twice the rotation frequency. Variation of the phase angle $\frac{1}{2}\pi - \sigma_r$ can be observed directly from the vibration trace if it is marked regularly twice per shaft revolution (through the use of two diametrically opposed datum marks on the shaft for instance). It has not proved difficult to devise electronic measuring techniques for these purposes.
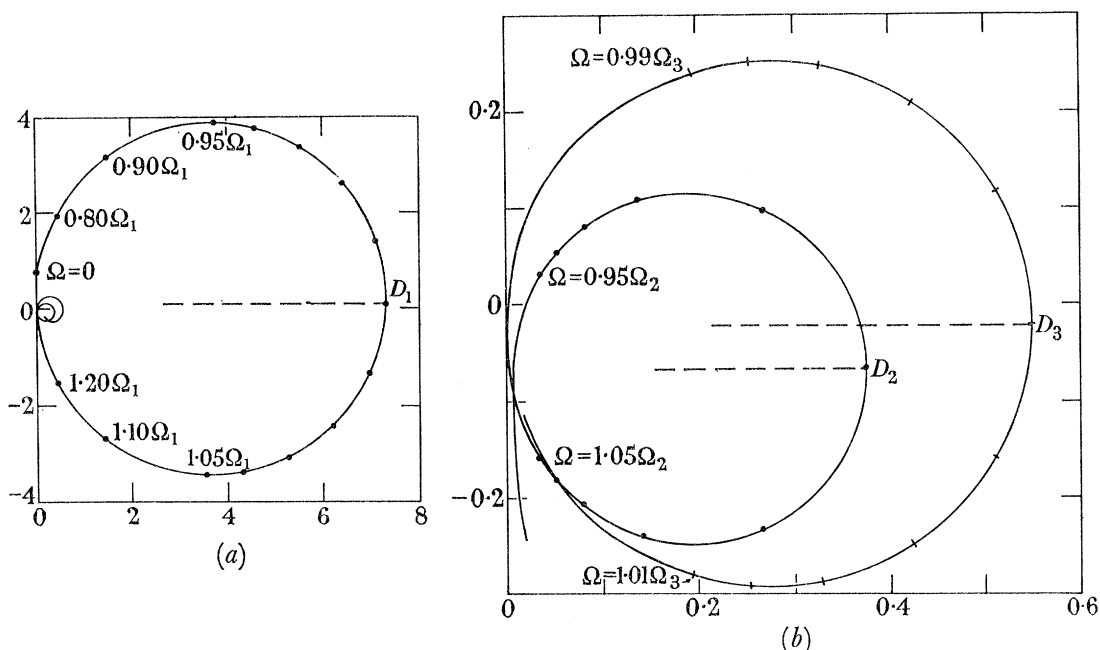

FIGURE 14. (a) Response in the first three modes. The unlabelled points · are plotted for $\Omega/\Omega_1 = 0.95$ (0.01) 1.05. (b) Enlargement of part of (a) showing response in the second and third modes. The points · are plotted for $\Omega/\Omega_2 = 0.95$ (0.01) 1.05 and the marks I for $\Omega/\Omega_3 = 0.990$ (0.002) 1.010.

It will be seen that all the modal components of the 'exciting force' $\bar{A}_r$ in equation (69) are in phase with each other (that is, for $r = 1, 2, \ldots$). This is reflected in the Argand diagram when $\xi_r^{(2)}$ is plotted since some fixed direction represents the direction of every modal component of the exciting force. Thus all the resonance diameters are parallel with each other.

The situation is best explained by means of an example. Figure 11 shows the first three characteristic functions for a uniform 'clamped-pinned' beam. Figures 14 and 15 display the variation of the response vectors with shaft speed Ω at points $x = 0.3l$ and $x = 0.8l$ respectively along the shaft as the speed is increased from a low value to a value above Ω_3.

The curves in figures 14 and 15 are calculated from the equation

$$\xi^{(2)} e^{-2i\Omega t} = \frac{g}{4\Omega_1^2} \left(\frac{\omega_r'^2 - \omega_r^2}{\omega_r'^2 + \omega_r^2}\right) \sum_{r=1}^{3} \frac{g_r}{g} \left(\frac{\Omega_1}{\Omega_r}\right)^2 \frac{i\,e^{-i\sigma_r}\phi_r(x)}{\sqrt{\left[\left(1 - \frac{\Omega^2}{\Omega_r^2}\right)^2 + \frac{\mu_r^2 \omega_r^{*2}\Omega^2}{\Omega_r^4}\right]}}. \tag{72}$$

The factor outside the summation sign is the same for all modal numbers r (see inequality

(21)) and so can be omitted as a scale factor. The value $\mu_1 = 0.05$ is used, μ_2 and μ_3 being calculated through relations (16). It can be seen that the resonance diameters in all three modes are parallel, although the diameters in the second modes are in opposite directions.
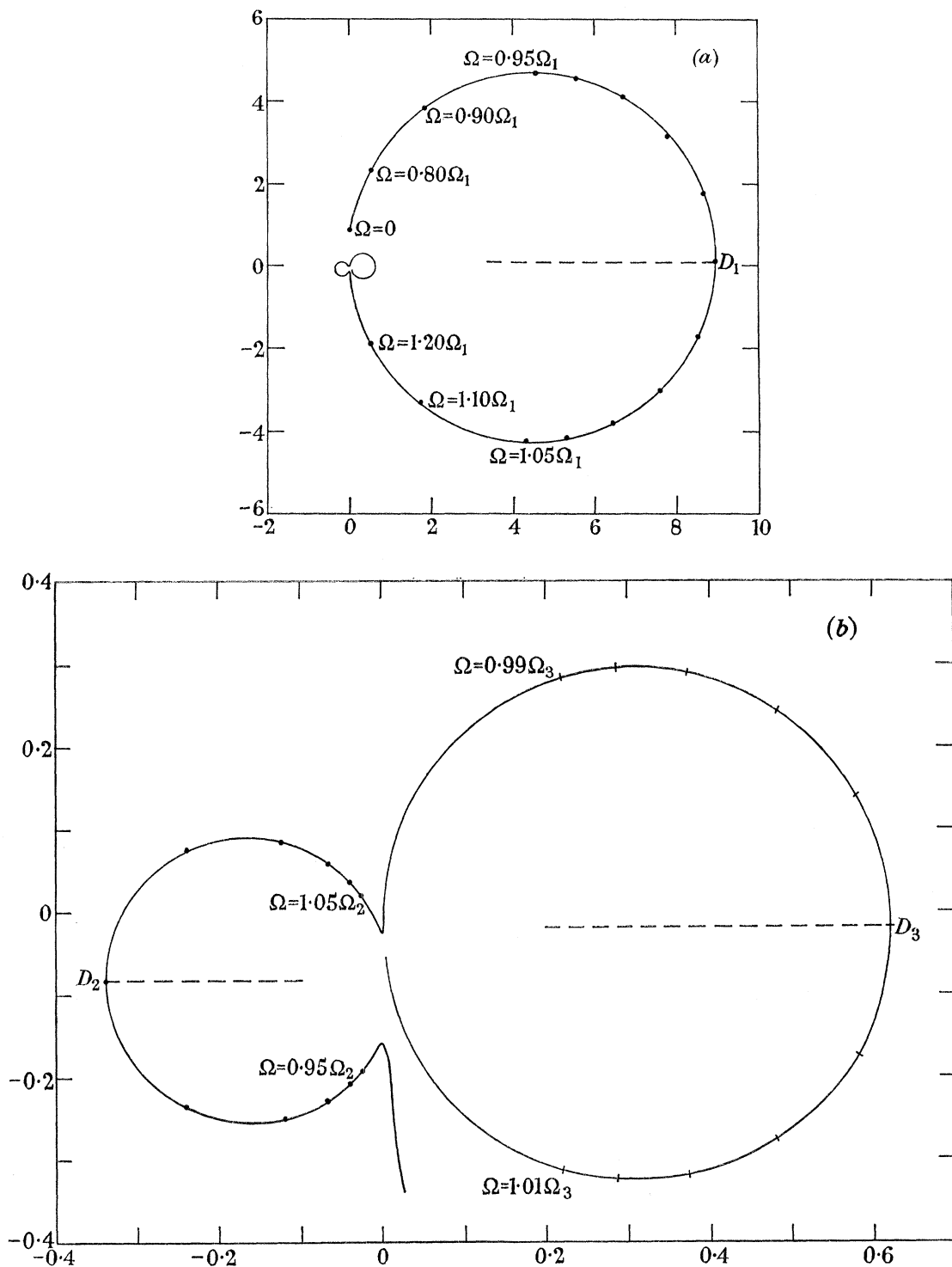

FIGURE 15. (a) Response in the first three modes. The unlabelled points · are plotted for $\Omega/\Omega_1 = 0.95$ (0.01) 1.05. (b) Enlargement of part of (a) showing response in the second and third modes. The points · are plotted for $\Omega/\Omega_2 = 0.95$ (0.01) 1.05 and the marks I for $\Omega/\Omega_3 = 0.900$ (0.002) 1.010.

In practice, therefore, one would monitor the amplitude and phase of the second order vibration as already mentioned. This response vector can be plotted on an Argand diagram and circular arcs fitted to the locus in regions where the frequency spacing suggests resonances (as, for example, near the points D_1, D_2 and D_3 in figures 14 and 15). The actual secondary critical speeds $\Omega_1, \Omega_2, \Omega_3, \ldots$ can be found by locating the points of maximum frequency spacing or by constructing the resonance diameters—parallel to the real axis—of the circular arcs. These diameters are the broken lines through the points D_1, D_2 and D_3 in figures 14 and 15. Alternatively the critical speeds $\Omega_1, \Omega_2, \Omega_3, \ldots$ are the speeds corresponding to those points on the locus whose distances from that axis through the origin which is perpendicular to the resonance diameters are local maxima. The accurate determination of these speeds from conventional 'amplitude peaks' is not easy; indeed the correct interpretation of amplitude peaks is often a matter of great difficulty.

INDUSTRIAL ROTORS

There is no longer any question of the importance of secondary vibration so far as large industrial rotors are concerned. Amplitudes of vibration of 0·005 in. or more have frequently been observed at the bearing pedestals and these are much too high to be allowable in service. For this reason various aspects of secondary vibration have been studied. For instance, it is desirable to discover what differential stiffness effects arise from the wedges that prevent electrical conductors from flying out. Again, it is common practice to attach by means of a rigid coupling an exciter to the opposite drive end of an alternator; how does the attachment of this exciter affect the double frequency vibration? Questions such as these are of considerable practical importance.

As might be expected, this type of research requires specialized study which can only be carried on in industry. Results are being accumulated rapidly and no doubt these will appear in the technical literature in due course. As this paper describes an analytical tool—the polar plot—with which this type of investigation can conveniently be made, however, it is not inappropriate to refer briefly to results taken from an actual rotor.

Figure 16 shows the polar representation of second order vibration for the two main bearings of a 350 MW alternator-rotor. The rotor was driven through a double Hooke joint and the horizontal transverse vibrations of the pedestals were monitored and measured as functions of rotation speed. The signal obtained in this way was filtered at twice the rotational frequency. The phase of the rotor distortion (which distortion, to a stationary observer, produces the 'vibration') was measured relative to a diametral (as opposed to 'radial') plane fixed in the rotor and revolving with it. Curves were drawn of amplitude and phase against speed and readings were thus obtained for regular 20 rev./min intervals. This procedure was adopted, as it would be difficult to take readings directly for accurately spaced speeds, because of the high polar moment of inertia of an alternator-rotor and the consequent difficulty of quickly imposing on it a predetermined speed.

The results to which figure 16 relates were in fact taken from an unwound rotor which had no exciter attached but which had iron in the pole faces, installed in continuous lengths. The results are for a limited speed range and were taken during the course of a research programme. Aside from the evident absence of instability, they seem quite reassuring in the

light of the foregoing theory. It will be seen that the following features are displayed by the curves, all of them in line with the predictions that have been made:

(1) Points corresponding to equal increments of speed 'open out' and 'close up'.

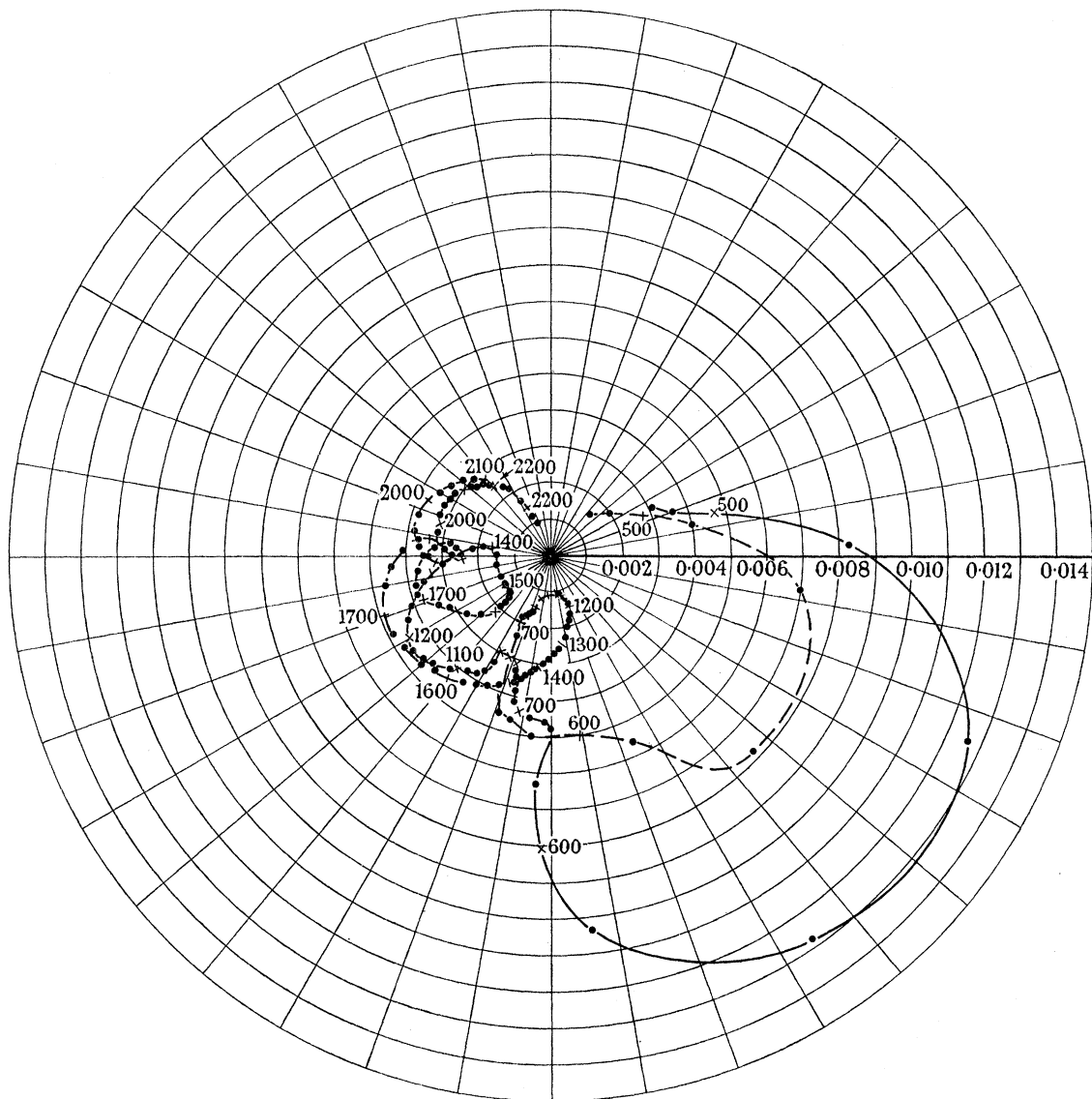(2) Where the points open out, the curve forms arcs that are approximately circular.

FIGURE 16. ———, Vibration of drive end bearing; – – – –, vibration of opposite drive end bearing. The points are labelled in rev/min and those marked · are plotted at intervals of 20 rev/min.

(3) The most obvious arcs are centred approximately on 550, 1700 and 2000 rev/min. If the two resonance diameters of the arcs at each of these speeds were constructed, they would be approximately parallel, showing that the pedestals are moving in phase in each of these modes. This would be expected in the odd numbered modes at half the critical speeds of odd order.

(4) The spacing opens out at about 1300 rev/min with the resonance diameters approximately in opposite directions, showing that the pedestals are moving approximately in

antiphase in this mode. This corresponds to a second mode oscillation and, as the theory predicts, the modal response is far smaller than that in the first mode (at 550 rev/min).

(5) All the resonance diameters are approximately parallel to one another; this seems plain at 550, 1300 and 2000 rev/min, but less clear at 1700 rev/min.

It is worth noting an interesting and potentially useful by-product of this form of analysis. It furnishes a means of accurately measuring critical speeds that are greater than the maximum permissible running speed. This provides useful checks on theoretical calculations of critical speeds (which calculations are still a matter of great difficulty, especially so far as the effects of bearings are concerned). Secondly, this information can well simplify the process of balancing modes whose critical speeds lie above the maximum permissible driving speed.

APPENDIX. CALCULATION OF THE FACTOR g_r

This appendix is concerned with the values of the modal components of the weight force described by the terms $g_1, g_2, g_3, \ldots$ which are defined in equation (36). Remembering relations (5), equation (36) can be rewritten in the following form

$$\frac{g_r}{g} = \frac{EI}{\omega_r^2 A\rho \, Z} \int_0^l \frac{\mathrm{d}^4 \phi_r}{\mathrm{d}x^4} \, \mathrm{d}x. \tag{73}$$

The expression for g_r can now be integrated readily to give

$$\frac{g_r}{g} = \frac{EI}{\omega_r^2 A\rho \, Z} \left[\frac{\mathrm{d}^3 \phi_r}{\mathrm{d}x^3}\right]_0^l = \frac{1}{Z}\left(\frac{l}{\lambda_r l}\right)\left[\frac{1}{\lambda_r^3}\frac{\mathrm{d}^3 \phi_r}{\mathrm{d}x^3}\right]_0^l, \tag{74}$$

in which we have substituted $\qquad \lambda_r^4 = \omega_r^2 A\rho / EI. \tag{75}$

The factors Z and $\lambda_r l$ and the functions $\lambda_r^{-3} \mathrm{d}^3 \phi_r / \mathrm{d}x^3$ have been tabulated by Bishop & Johnson (1960) for the lowest five modes of flexural vibration of uniform beams with 'ideal' end restraints. The factors $g_1, g_2, \ldots$ can thus be calculated readily and the results are listed in the accompanying table.

It should be noted that rigid body modes (see Gladwell, Bishop & Johnson 1962) are used in the appropriate calculations and in these cases equation (36) is integrated directly. Thus, for example, the first and second modes of a free–free beam are rigid body modes. The values of g_r derived from rigid body modes are marked accordingly in table 1.

TABLE 1. MODAL COMPONENTS OF WEIGHT FORCE FOR VARIOUS UNIFORM BEAMS

(* Denotes rigid body mode)

end conditions	g_1/g	g_2/g	g_3/g	g_4/g	g_5/g
clamped–clamped	0·83	0	0·36	0	0·23
pinned–pinned	1·27	0	0·42	0	0·25
clamped–pinned	0·86	0·08	0·33	0·04	0·21
clamped–free	0·78	0·43	0·25	0·18	0·14
clamped–sliding	0·83	0·36	0·23	0·17	0·13
pinned–sliding	1·27	−0·42	0·25	−0·18	0·14
sliding–sliding	1·41*	0	0	0	0
free–free	1·00*	0*	0	0	0
pinned–free	0·87*	0·37	−0·20	0·14	−0·11
sliding–free	1·00*	0	0	0	0

REFERENCES

Biezeno, C. B. & Grammel, R. 1954 *Engineering dynamics*. London: Blackie and Son Ltd.

Bishop, R. E. D. 1959 *J. Mech. Engng. Sci.* **1**, 50.

Bishop, R. E. D. & Gladwell, G. M. L. 1959 *J. Mech. Engng Sci.* **1**, 66.

Bishop, R. E. D. & Gladwell, G. M. L. 1963 *Phil. Trans.* A, **255**, 241.

Bishop, R. E. D. & Johnson, D. C. 1960 *Mechanics of vibration*, chap. 7. Cambridge University Press.

Bishop, R. E. D. & Parkinson, A. G. 1963 *Proc. Inst. Mech. Engrs, Lond.* **177**, 407.

Dick, J. 1948 *Phil. Mag.* (7), **39**, 946.

Dimentberg, F. M. 1961 *The flexural vibrations of rotating shafts*. London: Butterworth and Co.

Foote, W. R., Poritsky, H. & Slade, J. J. 1943 *J. Appl. Mech.* **10**, A-77.

Gladwell, G. M. L. & Bishop, R. E. D. 1959 *J. Mech. Engng Sci.* **1**, 78.

Gladwell, G. M. L., Bishop, R. E. D. & Johnson, D. C. 1962 *J. R. Aero. Soc.* **66**, 394.

Hull, E. H. 1961 *J. Engng for Industry*, **83**, 219.

Jeffcott, H. H. 1919 *Phil. Mag.* (6), **37**, 304.

Johnson, D. C. 1952 *Aircr. Engng*, **24**, 234.

Kellenberger, W. 1955 *Brown Boveri Rev.* **42**, 79.

Laffoon, C. M. & Rose, B. A. 1940 *Trans. Amer. Inst. Elect. Engrs*, **59**, 30.

Lindley, A. L. G. & Bishop, R. E. D. 1963 *Proc. Inst. Mech. Engrs, Lond.* **177**, 811.

Moore, L. S. & Dodd, E. G. 1964 *G.E.C. J.* **31**, 74.

Mortensen, S. H. & Ryan, J. J. 1940 *Trans. Amer. Inst. Elect. Engrs*, **59**, 51.

Parkinson, A. G. 1965 Ph.D. Thesis, University of London.

Parkinson, A. G. & Bishop, R. E. D. 1965 *J. Mech. Engng Sci.* **7**, 33.

Parkinson, A. G., Jackson, K. L. & Bishop, R. E. D. 1963 *J. Mech. Engng Sci.* **5**, 114.

Robertson, D. 1933 *Engineer, Lond.* **156**, 152, 179, 213.

Smith, D. M. 1933 *Proc. Roy. Soc.* A, **142**, 92.

Soderberg, C. R. 1932 *Trans. Amer. Soc. Mech. Engrs*, **54**, 45.

Taylor, H. D. 1940 *J. Appl. Mech.* **7**, A-71.

Tondl, A. 1958 *The vibration of rotors whose stiffnesses are unequal*. Bratislava: Slovenska Akademia Vied.
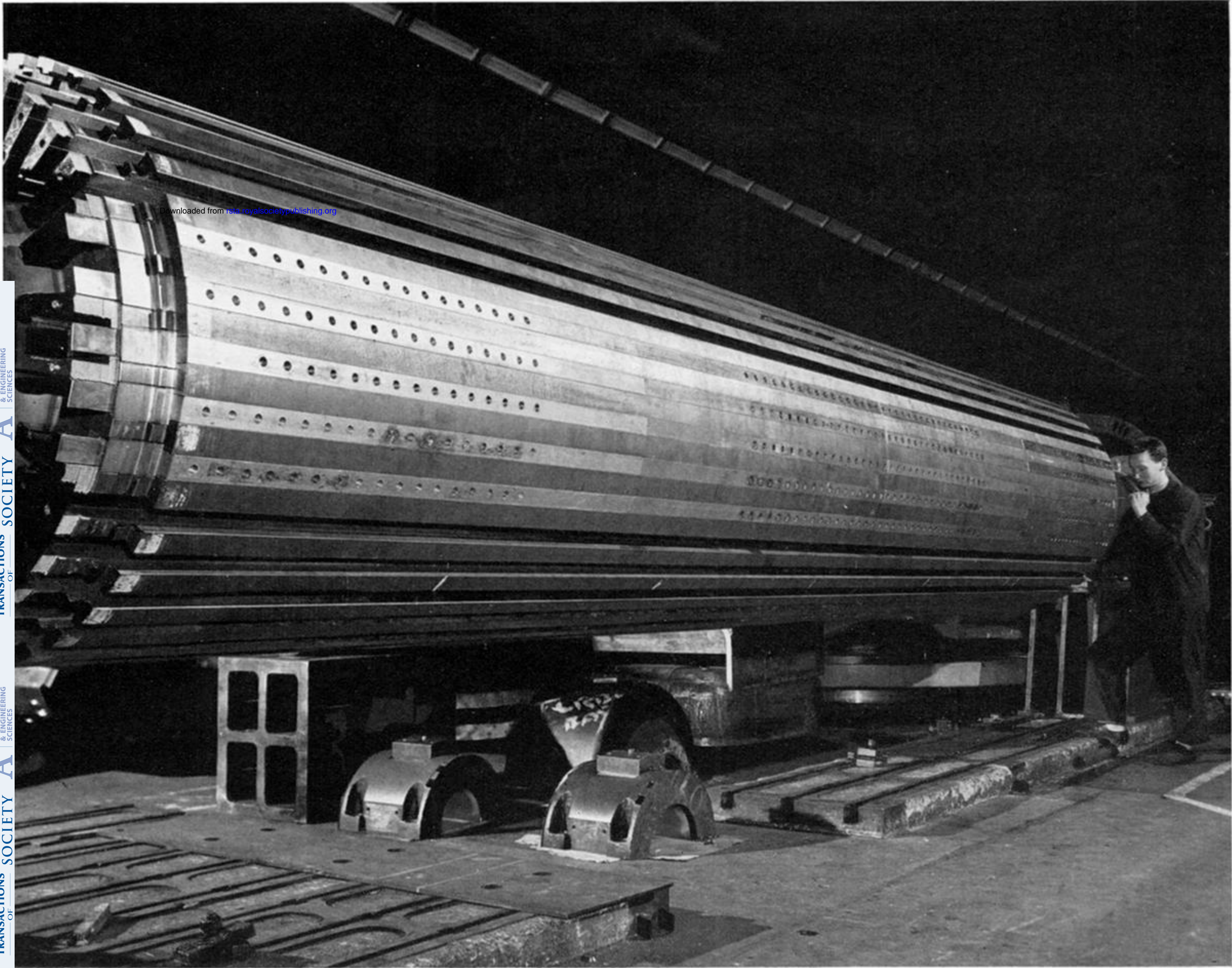
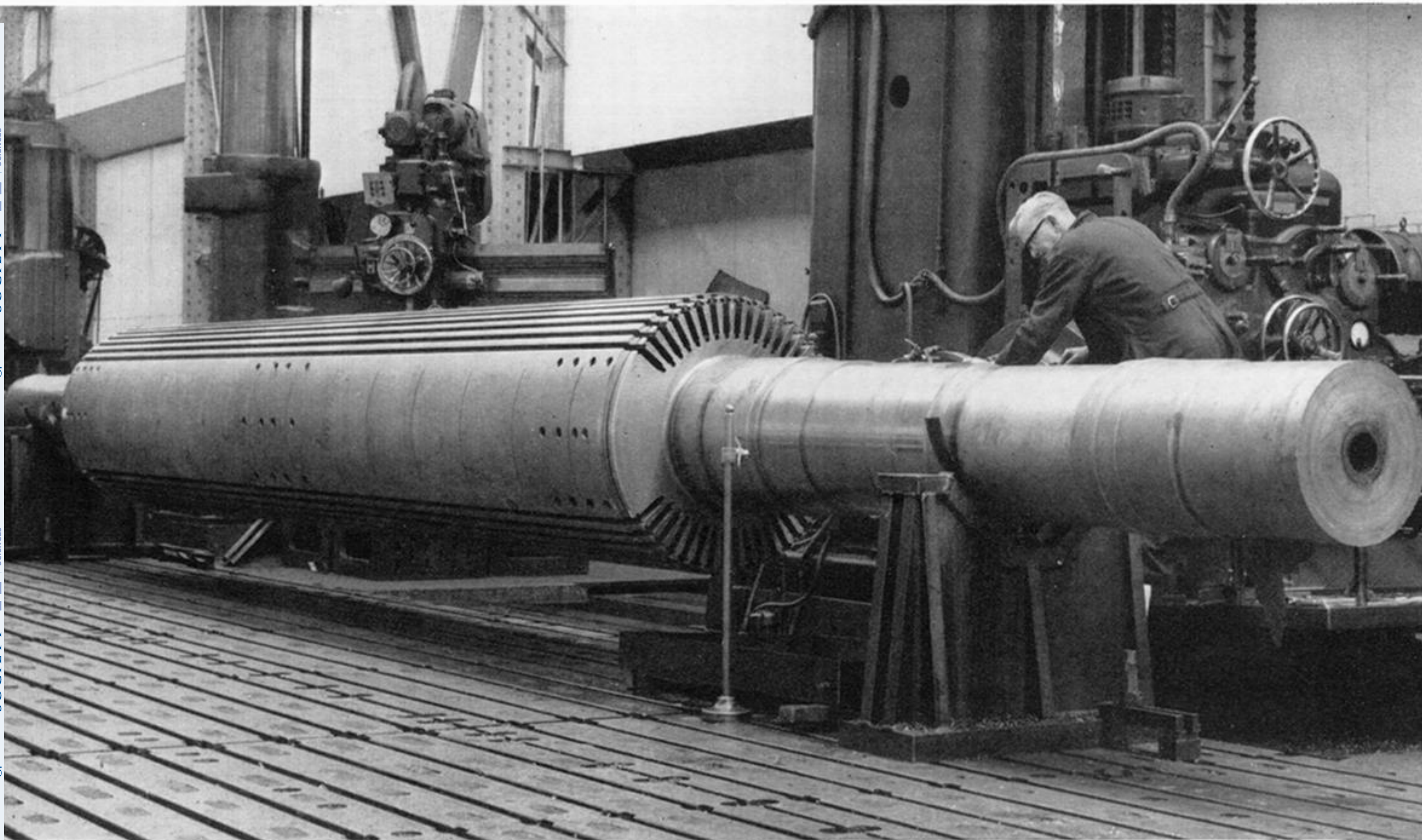FIGURE 3 (*a*). (By courtesy of General Electric Company, Witton.)

Figure 3(b). (By courtesy of English Electric Company, Stafford.)